

# On the Performance Bound of Sparse Estimation with Sensing Matrix Perturbation

Yujie Tang, Laming Chen, and Yuantao Gu

**Abstract**—This paper focusses on the sparse estimation in the situation where both the sensing matrix and the measurement vector are corrupted by additive Gaussian noises. The performance bound of sparse estimation is analyzed and discussed in depth. Two types of lower bounds, the constrained Cramér-Rao bound (CCRB) and the Hammersley-Chapman-Robbins bound (HCRB), are discussed. It is shown that the situation with sensing matrix perturbation is more complex than the one with only measurement noise. For the CCRB, its closed-form expression is deduced. It demonstrates a gap between the maximal and nonmaximal support cases. It is also revealed that a gap lies between the CCRB and the MSE of the oracle pseudoinverse estimator, but it approaches zero asymptotically when the problem dimensions tend to infinity. For a tighter bound, the HCRB, despite of the difficulty in obtaining a simple expression for general sensing matrix, a closed-form expression in the unit sensing matrix case is derived for a qualitative study of the performance bound. It is shown that the gap between the maximal and nonmaximal cases is eliminated for the HCRB. Numerical simulations are performed to verify the theoretical results in this paper.

**Index Terms**—Sparsity, unbiased estimation, constrained Cramér-Rao bound, Hammersley-Chapman-Robbins bound, sensing matrix perturbation, asymptotic behavior.

## I. INTRODUCTION

The problem of sparse recovery from linear measurement has been a hot topic these years and has drawn a great deal of attention. Various practical algorithms of sparse recovery have been proposed and theoretical results have been derived [1]–[10]. The theory of sparse recovery can be applied to various fields, especially the field of compressive sensing which considerably decreases the sampling rate of sparse signals [11]–[13].

Suppose that a sparse signal  $\mathbf{x} \in \mathbb{R}^n$  is observed through noisy linear measurement

$$\mathbf{y} = \mathbf{A}\mathbf{x} + \mathbf{n}, \quad (1)$$

where  $\mathbf{A} \in \mathbb{R}^{m \times n}$  is called the sensing matrix,  $\mathbf{y} \in \mathbb{R}^m$  is the measurement vector, and  $\mathbf{n} \in \mathbb{R}^m$  is the additive random noise vector. The main issue of sparse recovery is to estimate  $\mathbf{x}$  from measurement  $\mathbf{y}$  with estimation error as small as possible, and the recovery algorithm should be computationally tractable.

The performance of various recovery algorithms in noisy scenarios has been theoretical analyzed [6]–[8], [14]–[18]. Most of these works only consider the upper bound of the estimation error. Theoretical result about to what extent the

estimation error can be small (i.e. the theoretical lower bound of estimation error) is of great interest because it sets a limit performance which all sparse recovery algorithms cannot exceed. There are various approaches that try to handle this topic. Reference [19] employed a minimax approach to study the problem. Another approach is to reformulate the sparse recovery problem as a parameter estimation problem [20]. The sparse vector  $\mathbf{x}$  is viewed as a deterministic parameter vector, and  $\mathbf{y}$  represents the observation data. The goal of this approach is to minimize the mean-squared error  $E[(\hat{\mathbf{x}} - \mathbf{x})^2]$  (MSE) among all possible estimators  $\hat{\mathbf{x}} = \hat{\mathbf{x}}(\mathbf{y})$ . The theory of lower bounds of MSE has been well established for parameter vector  $\mathbf{x} \in \mathbb{R}^n$  without further constraints [21]. Various bounds, including the Cramér-Rao bound [21], [22], the Hammersley-Chapman-Robbins bound [23], and the Barankin bound [25], have been introduced. However, the classical theory in general requires some modification to adapt to the sparse settings.

Recently, researches on the lower bounds of MSE for constrained parameter vectors, especially sparse parameter vectors, have been developed. The Cramér-Rao bound has been modified for the constrained parameter case, and works well in the sparse settings [20], [26]. The Hammersley-Chapman-Robbins bound requires little essential modifications, and has also been applied to the the problem of sparse recovery [27], [28].

This paper also focusses on the theoretical lower bounds of sparse estimators and employs the constrained Cramér-Rao bound and the Hammersley-Chapman-Robbins bound, but deals with a more general setting in which the sensing matrix is perturbed by additive random noise. Perturbed sensing matrices appear in many practical scenarios, and therefore it is necessary to study the theoretical bounds of sparse recovery with perturbed sensing matrix [29]–[31]. One of the consequences of perturbed sensing matrix is that it is a kind of multiplicative noise, and the total noise on the measurement vector is dependent on the parameter vector  $\mathbf{x}$ , which demonstrates potential complexity compared to the sensing matrix perturbation-free setting (1).

The main contributions of this work are the theoretical bounds of sparse recovery with perturbed sensing matrix and noisy measurement vector. Closed-form expressions of the constrained CRB will be derived, and the quantitative behavior will be discussed. For the Hammersley-Chapman-Robbins bound, only the case of identity sensing matrix is studied for the sake of simplicity, but the results are still inspiring in that its analysis is much simpler and can still provide much information about the behavior of the theoretical

Yujie Tang, Laming Chen, and Yuantao Gu are with the Department of Electronic Engineering, Tsinghua University, Beijing 100084, China (E-mail: gyt@tsinghua.edu.cn).

lower bounds when the noises are large.

The rest of this paper is organized as follows. In Section II, the fundamental problem of sparse recovery with perturbed sensing matrix is introduced, and the classical theory of parameter estimation will be reviewed. In Section III, the constrained Cramér-Rao bound will be derived, and quantitative analysis will be provided in order to have a deeper understanding of its behavior. In Section IV, the Hammersley-Chapman-Robbins bound will be derived for the case with unit sensing matrix, and its behavior with different settings of signals and noises will also be studied. In Section V, numerical results will be presented to verify the theoretical results. This paper is concluded in Section VI and the proofs are postponed to Appendices.

### Notation

The  $M \times M$  identity matrix is denoted by  $\mathbf{U}_M$ . For any index set  $\Lambda \subset \{1, 2, \dots, N\}$ ,  $|\Lambda|$  denotes the cardinality, i.e. the number of elements of  $\Lambda$ , and  $\Lambda^c$  denotes the complement set  $\{1, 2, \dots, N\} \setminus \Lambda$ . For any index set  $\Lambda$  and any  $N$ -dimensional vector  $\mathbf{v}$  ( $N \geq |\Lambda|$ ),  $\mathbf{v}_\Lambda$  denotes the  $|\Lambda|$ -length vector containing the entries of  $\mathbf{v}$  indexed by  $\Lambda$ . For any index set  $\Lambda$  and any  $M \times N$  matrix  $\mathbf{M}$  ( $N \geq |\Lambda|$ ),  $\mathbf{M}_\Lambda$  denotes the  $M \times |\Lambda|$  matrix containing the columns of  $\mathbf{M}$  corresponding to  $\Lambda$ . For any vector  $\mathbf{v}$ ,  $\|\mathbf{v}\|_{\ell_p}$  denotes the  $p$ -norm of  $\mathbf{v}$ . For any appropriate matrix  $\mathbf{M}$ ,  $\mathbf{M}^\dagger$  denotes the Moore-Penrose pseudo-inverse of  $\mathbf{M}$ . For  $\mathbf{x} = (x_1, \dots, x_N)^\top$ ,  $\nabla_{\mathbf{x}}$  denotes the gradient operator  $(\partial/\partial x_1, \dots, \partial/\partial x_N)^\top$ , and  $\nabla_{\mathbf{x}}^\top$  denotes its transposition.  $\mathbf{e}_k$  denotes the  $k$ th column vector of the identity matrix.  $\mathcal{N}(\boldsymbol{\mu}, \boldsymbol{\Sigma})$  denotes (multidimensional) Gaussian distribution with mean  $\boldsymbol{\mu}$  and covariance  $\boldsymbol{\Sigma}$ . Other notations will be introduced when needed.

## II. PROBLEM SETTING

The fundamental background of sparse estimation with general perturbation, i.e. where both sensing matrix perturbation and measurement noise exist, is introduced in this section. In the case of general perturbation, the measurement vector is observed via a corrupted sensing matrix as

$$\mathbf{y} = (\mathbf{A} + \mathbf{E})\mathbf{x} + \mathbf{n}, \quad (2)$$

where  $\mathbf{x}$  is the deterministic parameter to be estimated, and  $\mathbf{y}$  is the measurement vector.  $\mathbf{E} \in \mathbb{R}^{m \times n}$  represents the perturbation on the sensing matrix, whose elements are i.i.d. Gaussian distributed random variables with zero mean and variance  $\sigma_e^2$ . The vector  $\mathbf{n} \sim \mathcal{N}(0, \sigma_n^2 \mathbf{U}_m)$  is the noise on the measurement vector  $\mathbf{y}$ , and is independent of  $\mathbf{E}$ .

The parameter  $\mathbf{x}$  is supposed to be sparse, i.e. the size of its support is far less than its dimension. The support of  $\mathbf{x}$  is denoted by  $S$ , and its size is assumed not to be greater than  $s$ , i.e.

$$|S| = \|\mathbf{x}\|_{\ell_0} \leq s. \quad (3)$$

Furthermore, it is adopted in the following text that

$$\text{spark}(\mathbf{A}) > 2s, \quad (4)$$

where  $\text{spark}(\mathbf{A})$  is defined as the smallest possible number  $k$  such that there exists a subgroup of  $k$  columns from  $\mathbf{A}$  that

are linearly dependent [32]. The above prerequisite ensures that two different  $s$ -sparse signals will not share the same measurement vector if the measurement is precise.

An estimator  $\hat{\mathbf{x}} = \hat{\mathbf{x}}(\mathbf{y})$  is a function of the measurement vector, and is essentially a random variable. It is demanded that a good estimator should approximate the parameter  $\mathbf{x}$  as accurately as possible. A widely used criterion of the precision of an estimator is the mean square error (MSE), given by

$$\text{mse}(\hat{\mathbf{x}}) = E_{\mathbf{y};\mathbf{x}}[\|\hat{\mathbf{x}}(\mathbf{y}) - \mathbf{x}\|_{\ell_2}^2]. \quad (5)$$

Here,  $E_{\mathbf{y};\mathbf{x}}[\cdot]$  denotes the expectation taken with respect to the pdf  $p(\mathbf{y}; \mathbf{x})$  of the measurement  $\mathbf{y}$  parameterized by  $\mathbf{x}$ . Note that the MSE is in general dependent on  $\mathbf{x}$ .

### A. Review of Unbiasedness and the Barankin bound

In order to obtain a good estimator, one usually resorts to the following optimization problem:

$$\arg \min_{\hat{\mathbf{x}}(\cdot)} \text{mse}(\hat{\mathbf{x}}) = \arg \min_{\hat{\mathbf{x}}(\cdot)} E_{\mathbf{y};\mathbf{x}}[\|\hat{\mathbf{x}}(\mathbf{y}) - \mathbf{x}\|_{\ell_2}^2],$$

and hopes that its solution could provide an estimator that achieves the minimum MSE globally. However, if no restrictions are imposed on the estimators, the solution of the above problem is trivially  $\hat{\mathbf{x}}(\mathbf{y}) = \mathbf{x}$ , which achieves the minimum MSE (zero) only at one specific parameter value. This shows that the globally best estimator does not exist. Therefore one should take into account the proper restrictions imposed on the estimators.

One widely used type of restrictions on estimators is unbiasedness. Unbiased estimators are the ones that satisfy

$$E_{\mathbf{y};\mathbf{x}}[\hat{\mathbf{x}}(\mathbf{y})] = \mathbf{x}, \quad \forall \mathbf{x} \in \mathcal{X}. \quad (6)$$

Here  $\mathcal{X}$  denotes the set of all possible values of the parameter  $\mathbf{x}$ . In the sparse setting, the notation  $\mathcal{X}_s$  is used for this set and could be formulated as

$$\mathcal{X}_s = \{\mathbf{x} \in \mathbb{R}^n : \|\mathbf{x}\|_{\ell_0} \leq s\}. \quad (7)$$

The set of all unbiased estimators will be denoted by  $\mathcal{U}$ .

While unbiasedness excludes trivial estimators such as  $\hat{\mathbf{x}}(\mathbf{y}) = \mathbf{x}_1$  for some specific  $\mathbf{x}_1$ , it is still not guaranteed that there exists a uniformly minimum variance unbiased (UMVU) estimator, i.e. an unbiased estimator that achieves the minimum MSE globally among all the unbiased estimators. For the case where the sensing matrix perturbation vanishes, it has already been proved that the UMVU does not exist when  $s < n$  [20]. Despite the fact that the UMVU estimator may not exist, one can still solve the following minimization problem

$$\arg \min_{\hat{\mathbf{x}}(\cdot) \in \mathcal{U}} \text{mse}(\hat{\mathbf{x}}) = \arg \min_{\hat{\mathbf{x}}(\cdot) \in \mathcal{U}} E_{\mathbf{y};\mathbf{x}}[\|\hat{\mathbf{x}}(\mathbf{y}) - \mathbf{x}\|_{\ell_2}^2] \quad (8)$$

for each  $\mathbf{x} \in \mathcal{X}_s$  separately. The solution of the above minimization problem for a specific  $\mathbf{x}$  is called a locally minimum variance unbiased (LMVU) estimator, and its MSE is known as the Barankin bound (BB) [25]. The BB can be viewed as the lower bound of the MSE of all unbiased estimators. Unfortunately, the BB often does not possess a

closed-form expression; even in the case where the closed-form expression exists, the computation is usually of great complexity.

In the remainder of this paper, two types of lower bounds of the BB, the constrained Cramér-Rao bound (CCRB) and the Hammersley-Chapman-Robbins bound (HCRB), are discussed for sparse estimation with general perturbation. As they are lower bounds of the BB, they can also be viewed as the lower bounds of the MSE of unbiased estimators. Although they are not as tight as the BB, they usually possess simpler expressions and can provide insights into the properties of the BB.

### III. THE CONSTRAINED CRB

In this section, the constrained Cramér-Rao bound (CCRB) of the estimation problem (2) is considered. The CCRB generalizes the original CRB to the case where the parameter is constrained in an arbitrary given set. Researches on CCRB have been developed recently and especially on the situation of sparse estimation [20], [26]. The CCRB can be summarized by the following proposition.

*Proposition 1:* [26] Suppose that the parameter  $\mathbf{x} \in \mathbb{R}^n$  lies in a given set  $\mathcal{X}^1$ , and  $\mathbf{x}_0$  is a specific value of  $\mathbf{x}$ . Define the set  $\mathcal{F}(\mathbf{x}_0)$  as follows,

$$\mathcal{F}(\mathbf{x}_0) = \{\mathbf{v} \in \mathbb{R}^n : \exists \epsilon_0(\mathbf{v}) > 0 \\ \text{s.t. } \forall \epsilon \in (0, \epsilon_0(\mathbf{v})), \mathbf{x}_0 + \epsilon \mathbf{v} \in \mathcal{X}\}.$$

It can be proved that  $\mathcal{F}(\mathbf{x}_0)$  is a subspace of  $\mathbb{R}^n$ . Let  $\mathbf{V} = [\mathbf{v}_1, \dots, \mathbf{v}_l]$  be an orthogonal basis of  $\mathcal{F}(\mathbf{x}_0)$ , and  $\mathbf{J}$  be the Fisher information matrix (FIM),

$$\mathbf{J}(\mathbf{x}_0) = E_{\mathbf{y}; \mathbf{x}_0} [(\nabla_{\mathbf{x}} \ln p(\mathbf{y}; \mathbf{x})) (\nabla_{\mathbf{x}}^T \ln p(\mathbf{y}; \mathbf{x}))]. \quad (9)$$

If

$$\mathcal{R}(\mathbf{V}\mathbf{V}^T) \subseteq \mathcal{R}(\mathbf{V}\mathbf{V}^T \mathbf{J} \mathbf{V}\mathbf{V}^T), \quad (10)$$

where  $\mathcal{R}(\mathbf{P})$  is the column space of  $\mathbf{P}$ , then for any estimator  $\hat{\mathbf{x}}$  which is unbiased in the neighborhood of  $\mathbf{x}_0$ , its covariance matrix  $\text{Cov}(\hat{\mathbf{x}})$  satisfies

$$\text{Cov}(\hat{\mathbf{x}}) \succeq \mathbf{V}(\mathbf{V}^T \mathbf{J} \mathbf{V})^\dagger \mathbf{V}^T, \quad (11)$$

where  $\mathbf{P} \succeq \mathbf{Q}$  means that  $\mathbf{P} - \mathbf{Q}$  is positive semidefinite. The trace of the covariance matrix gives the MSE of the estimator. Conversely, if (10) does not hold, then there exists no finite variance estimator which is unbiased in the neighborhood of  $\mathbf{x}_0$ .

*Remark 1:* Note that the estimators considered in Proposition 1 are “unbiased in the neighborhood of  $\mathbf{x}_0$ ”, which can be rigorously formulated as follows: define  $b(\mathbf{x}) = E[\hat{\mathbf{x}} - \mathbf{x}]$  to be the bias at  $\mathbf{x}$ , then one says that the estimator  $\hat{\mathbf{x}}$  is unbiased in the neighborhood of  $\mathbf{x}_0$  if and only if

$$\forall \mathbf{v} \in \mathcal{F}(\mathbf{x}_0), \quad b(\mathbf{x}_0) = 0 \text{ and } \left. \frac{\partial b(\mathbf{x})}{\partial \mathbf{v}} \right|_{\mathbf{x}_0} = 0. \quad (12)$$

<sup>1</sup>There are certain requirements that  $\mathcal{X}$  has to meet. Refer to [20] for detailed exposition. Fortunately, the set  $\mathcal{X}_s$  of the sparse setting meets all the requirements.

We denote the set containing all the estimators unbiased in the neighborhood of  $\mathbf{x}_0$  as  $\mathcal{U}_{\mathbf{x}_0}$ . In the sparse setting, it can be seen that

$$\mathcal{U} \subset \mathcal{U}_{\mathbf{x}_0}, \quad \forall \mathbf{x}_0 \in \mathcal{X}_s, \quad (13)$$

therefore the CCRB is certainly lower than the BB. Nevertheless, the CCRB has simple closed-form expression which is convenient to analyze. In this section we relax our restrictions on the estimators to be unbiased in the neighborhood of a specific parameter value.

From Proposition 1, it can be seen that the computation of CCRB mainly relies on the computation of the FIM  $\mathbf{J}$  and the orthogonal basis  $\mathbf{V}$ . The FIM  $\mathbf{J}$  is given by the following lemma.

*Lemma 1:* The Fisher information matrix is given by

$$\mathbf{J}(\mathbf{x}) = \frac{1}{\sigma_{\mathbf{x}}^2} \left[ \mathbf{A}^T \mathbf{A} + 2m\sigma_e^4 \frac{\mathbf{x}\mathbf{x}^T}{\sigma_{\mathbf{x}}^2} \right], \quad (14)$$

where  $\sigma_{\mathbf{x}}^2$  is defined as

$$\sigma_{\mathbf{x}}^2 = \sigma_e^2 \|\mathbf{x}\|_{\ell_2}^2 + \sigma_n^2. \quad (15)$$

*Proof:* The proof is postponed to Appendix A.  $\square$

Next we deal with the orthogonal basis  $\mathbf{V}$  of the subspace  $\mathcal{F}$ . The cases in which  $\|\mathbf{x}\|_{\ell_0} = s$  and  $\|\mathbf{x}\|_{\ell_0} < s$  should be discussed separately. For the case  $\|\mathbf{x}\|_{\ell_0} = s$ , it can be seen that for every  $k \in S = \text{supp}(\mathbf{x})$ , one has  $\|\mathbf{x} + \epsilon \mathbf{e}_k\|_{\ell_0} \leq s$ , i.e.  $\mathbf{x} + \epsilon \mathbf{e}_k \in \mathcal{X}_s$  for arbitrary  $\epsilon$ , and therefore  $\mathbf{e}_k \in \mathcal{F}$ ; on the other hand, for  $k \notin S$ , one has  $\|\mathbf{x} + \epsilon \mathbf{e}_k\|_{\ell_0} > s$  and thus  $\mathbf{e}_k \notin \mathcal{F}$ . It follows that the subspace  $\mathcal{F}(\mathbf{x})$  can be formulated as

$$\mathcal{F}(\mathbf{x}) = \text{span}(\{\mathbf{e}_{S_1}, \dots, \mathbf{e}_{S_s}\}), \quad (16)$$

in which  $S_1, \dots, S_s$  are the elements of the support  $S = \text{supp}(\mathbf{x})$ , and the basis  $\mathbf{V}$  can take the following form

$$\mathbf{V} = [\mathbf{e}_{S_1}, \dots, \mathbf{e}_{S_s}]. \quad (17)$$

For the case  $\|\mathbf{x}\|_{\ell_0} < s$ , the situation is rather different, because for every  $\mathbf{e}_k$ ,  $k = 1, \dots, n$ , one has  $\|\mathbf{x} + \epsilon \mathbf{e}_k\|_{\ell_0} \leq s$ . Thus it can be concluded that  $\mathcal{F}(\mathbf{x}) = \mathbb{R}^n$  in this case, and the basis  $\mathbf{V}$  can be given by  $[\mathbf{e}_1, \dots, \mathbf{e}_n] = \mathbf{U}_n$ .

With the form of the FIM  $\mathbf{J}$  and the basis  $\mathbf{V}$ , one can readily derive the CCRB of the problem (2). The situation in which  $\mathbf{x}$  has maximal support ( $\|\mathbf{x}\|_{\ell_0} = s$ ) is first analyzed.

*Theorem 1:* For  $\|\mathbf{x}\|_{\ell_0} = s$ , the CCRB is given by

$$\sigma_{\mathbf{x}}^2 \left[ \text{tr}((\mathbf{A}_S^T \mathbf{A}_S)^{-1}) - \frac{2m\sigma_e^4 \|(\mathbf{A}_S^T \mathbf{A}_S)^{-1} \mathbf{x}_S\|_{\ell_2}^2}{\sigma_{\mathbf{x}}^2 + 2m\sigma_e^4 \mathbf{x}_S^T (\mathbf{A}_S^T \mathbf{A}_S)^{-1} \mathbf{x}_S} \right], \quad (18)$$

where  $\sigma_{\mathbf{x}}^2$  is defined in (15).

*Proof:* The condition (10) should be checked first. The matrix  $\mathbf{V}^T \mathbf{J} \mathbf{V}$  is given by

$$\begin{aligned} \mathbf{V}^T \mathbf{J} \mathbf{V} &= \mathbf{V}^T \cdot \frac{1}{\sigma_{\mathbf{x}}^2} \left[ \mathbf{A}^T \mathbf{A} + 2m\sigma_e^4 \frac{\mathbf{x}\mathbf{x}^T}{\sigma_{\mathbf{x}}^2} \right] \cdot \mathbf{V} \\ &= \frac{1}{\sigma_{\mathbf{x}}^2} \left[ \mathbf{V}^T \mathbf{A}^T \mathbf{A} \mathbf{V} + 2m\sigma_e^4 \frac{\mathbf{V}^T \mathbf{x} \mathbf{x}^T \mathbf{V}}{\sigma_{\mathbf{x}}^2} \right] \\ &= \frac{1}{\sigma_{\mathbf{x}}^2} \left[ \mathbf{A}_S^T \mathbf{A}_S + 2m\sigma_e^4 \frac{\mathbf{x}_S \mathbf{x}_S^T}{\sigma_{\mathbf{x}}^2} \right]. \end{aligned}$$

Because we have assumed that  $\text{spark}(\mathbf{A}) > 2s$ , it follows that  $\mathbf{A}_S$  has full column rank, and thus  $\mathbf{V}^T \mathbf{J} \mathbf{V}$  is invertible by employing the Sherman-Morrison formula [33], which gives

$$(\mathbf{V}^T \mathbf{J} \mathbf{V})^{-1} = \sigma_{\mathbf{x}}^2 \left[ (\mathbf{A}_S^T \mathbf{A}_S)^{-1} - \frac{2m\sigma_e^4 (\mathbf{A}_S^T \mathbf{A}_S)^{-1} \mathbf{x}_S \mathbf{x}_S^T (\mathbf{A}_S^T \mathbf{A}_S)^{-1}}{\sigma_{\mathbf{x}}^2 + 2m\sigma_e^4 \mathbf{x}_S^T (\mathbf{A}_S^T \mathbf{A}_S)^{-1} \mathbf{x}_S} \right], \quad (19)$$

and thus  $\mathcal{R}(\mathbf{V} \mathbf{V}^T \mathbf{J} \mathbf{V} \mathbf{V}^T) = \mathcal{R}(\mathbf{V} \mathbf{V}^T)$ , i.e. the CCRB exists. The expression of the CCRB can also be obtained from (19) that

$$\begin{aligned} \text{mse}(\hat{\mathbf{x}}) &\geq \text{tr}(\mathbf{V}(\mathbf{V}^T \mathbf{J} \mathbf{V})^{-1} \mathbf{V}^T) \\ &= \text{tr}(\mathbf{V}^T \mathbf{V}(\mathbf{V}^T \mathbf{J} \mathbf{V})^{-1}) = \text{tr}((\mathbf{V}^T \mathbf{J} \mathbf{V})^{-1}) \\ &= \sigma_{\mathbf{x}}^2 \left[ \text{tr}((\mathbf{A}_S^T \mathbf{A}_S)^{-1}) - \frac{2m\sigma_e^4 \|(\mathbf{A}_S^T \mathbf{A}_S)^{-1} \mathbf{x}_S\|_{\ell_2}^2}{\sigma_{\mathbf{x}}^2 + 2m\sigma_e^4 \mathbf{x}_S^T (\mathbf{A}_S^T \mathbf{A}_S)^{-1} \mathbf{x}_S} \right]. \end{aligned} \quad (20)$$

□

Next consider the case in which  $\mathbf{x}$  has nonmaximal support. The CCRB of this case can be summarized as the following theorem.

*Theorem 2:* For  $\|\mathbf{x}\|_{\ell_0} < s$ , if the FIM  $\mathbf{J}$  is nonsingular, then the CCRB exists. Furthermore, if  $\mathbf{A}$  has full column rank, then the CCRB is given by

$$\sigma_{\mathbf{x}}^2 \left[ \text{tr}((\mathbf{A}^T \mathbf{A})^{-1}) - \frac{2m\sigma_e^4 \|(\mathbf{A}^T \mathbf{A})^{-1} \mathbf{x}\|_{\ell_2}^2}{\sigma_{\mathbf{x}}^2 + 2m\sigma_e^4 \mathbf{x}^T (\mathbf{A}^T \mathbf{A})^{-1} \mathbf{x}} \right]. \quad (21)$$

If the FIM  $\mathbf{J}$  is singular, then there do not exist finite variance estimators that are unbiased in the neighborhood of  $\mathbf{x}$ .

*Proof:* Because in this case  $\mathbf{V} = \mathbf{U}_n$ , the two subspaces are respectively  $\mathcal{R}(\mathbf{V} \mathbf{V}^T) = \mathbb{R}^n$  and  $\mathcal{R}(\mathbf{V} \mathbf{V}^T \mathbf{J} \mathbf{V} \mathbf{V}^T) = \mathcal{R}(\mathbf{J})$ . Therefore when  $\mathbf{J}$  is invertible, it can be seen that the condition (10) holds, and the CCRB can be obtained by taking the trace of  $\mathbf{J}^{-1}$ . In the special case where  $\mathbf{A}$  has full column rank, the inverse  $\mathbf{J}^{-1}$  can be calculated with the help of the Sherman-Morrison formula [33],

$$\mathbf{J}^{-1} = \sigma_{\mathbf{x}}^2 \left[ (\mathbf{A}^T \mathbf{A})^{-1} - \frac{2m\sigma_e^4 (\mathbf{A}^T \mathbf{A})^{-1} \mathbf{x} \mathbf{x}^T (\mathbf{A}^T \mathbf{A})^{-1}}{\sigma_{\mathbf{x}}^2 + 2m\sigma_e^4 \mathbf{x}^T (\mathbf{A}^T \mathbf{A})^{-1} \mathbf{x}} \right], \quad (22)$$

and the CCRB is

$$\begin{aligned} \text{mse}(\hat{\mathbf{x}}) &\geq \text{tr}(\mathbf{J}^{-1}) \\ &= \sigma_{\mathbf{x}}^2 \left[ \text{tr}((\mathbf{A}^T \mathbf{A})^{-1}) - \frac{2m\sigma_e^4 \|(\mathbf{A}^T \mathbf{A})^{-1} \mathbf{x}\|_{\ell_2}^2}{\sigma_{\mathbf{x}}^2 + 2m\sigma_e^4 \mathbf{x}^T (\mathbf{A}^T \mathbf{A})^{-1} \mathbf{x}} \right]. \end{aligned} \quad (23)$$

When  $\mathbf{J}$  is not invertible, the dimension of the column space of  $\mathbf{J}$  is less than  $n$ . Thus the condition (10) does not hold, and estimators that are unbiased in the neighborhood of  $\mathbf{x}$  do not exist. □

Theorem 2 illustrates that for the nonmaximal support case, the prior information of sparsity cannot lower the theoretical bound of estimation error compared to the ordinary problem where  $\mathbf{x}$  can be any vector in  $\mathbb{R}^n$ . This demonstrates a gap between the maximal and nonmaximal support cases of the CCRB, which is the main topic of the next subsection.

#### A. Gap between the Maximal and the Nonmaximal Cases

The gap between the maximal and nonmaximal cases of the CCRB can be revealed from the following example. Suppose we observe a sparse vector  $\mathbf{x} \in \mathcal{X}_s$  with  $s$  nonzero entries. Then by the result of Theorem 1, the CCRB is given by (18). Next we assume that one of the nonzero components, say  $x_q$ , tends to zero. Consequently, the CCRB given by (18) tends to a specific limit  $\gamma_1$ . However, when  $x_q$  equals zero, the CCRB cannot be computed by (18) anymore because its support is now nonmaximal, therefore the CCRB of the  $x_q = 0$  case is given by (21), which we temporarily denote as  $\gamma_2$ . It is interesting to find that  $\gamma_1$  and  $\gamma_2$  are not equal to each other, which means that the CCRB is not a continuous function of the parameter  $\mathbf{x}$ .

Generally one has  $\gamma_1 \leq \gamma_2$ , which can be inferred as follows.  $\gamma_1$  could be seen as the CRB of estimators which are unbiased on the subspace  $\text{span}(\{\mathbf{e}_i : i \in \text{supp}(\mathbf{x})\})$ , while  $\gamma_2$  could be seen as the CRB of estimators unbiased on  $\mathbb{R}^n$ . If the former class of estimators is denoted by  $\mathcal{U}_1$ , and the latter is denoted by  $\mathcal{U}_2$ , it can be seen that  $\mathcal{U}_1 \supset \mathcal{U}_2$ , and thus the lower bounds of estimation error of the two classes should satisfy  $\gamma_1 \leq \gamma_2$ . This conclusion can also be verified by numerical approaches.

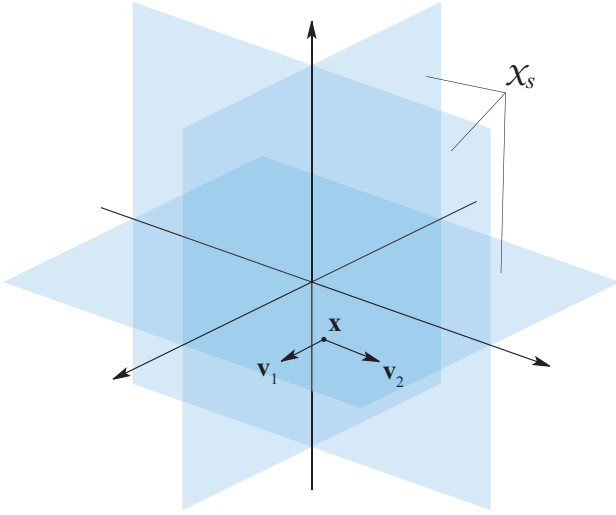
This gap originates from the “discontinuity” of the restriction that the estimator should be unbiased in the neighborhood of a specific parameter value. The “neighborhood” of a parameter point having maximal support in  $\mathcal{X}_s$  has an entirely different structure from that of a parameter point having nonmaximal support: the former is a subspace that is locally identical to  $\mathbb{R}^s$ , while the latter is a union of  $s$ -dimensional subspaces. Fig. 1 is a geometric illustration of the structure of the neighborhood of  $\mathbf{x}$ . It can be seen that as  $x_q \rightarrow 0$ , the structure of the neighborhood of  $\mathbf{x}$  will have an abrupt change: from being locally identical to  $\mathbb{R}^s$  to being locally identical to  $\mathbb{R}^n$ . This is the cause of the gap between the maximal and nonmaximal cases.

On the other hand, if a stronger condition, global unbiasedness, is imposed on the considered estimators instead of unbiasedness in the neighborhood, i.e. the estimators are restricted to be unbiased for all  $\mathbf{x} \in \mathcal{X}_s$ , then this discontinuity should not occur. Thus the corresponding lower bound should also be continuous as  $x_q \rightarrow 0$ , i.e.  $\mathbf{x}$  changes from having maximal support to having nonmaximal support. Since  $\gamma_1 \leq \gamma_2$ , it is further demonstrated that the CCRB for maximal support is not sufficiently tight for estimators in  $\mathcal{U}$ , especially when the support of  $\mathbf{x}$  is nearly nonmaximal, i.e. at least one of the non-zero entries is small compared to other non-zero entries.

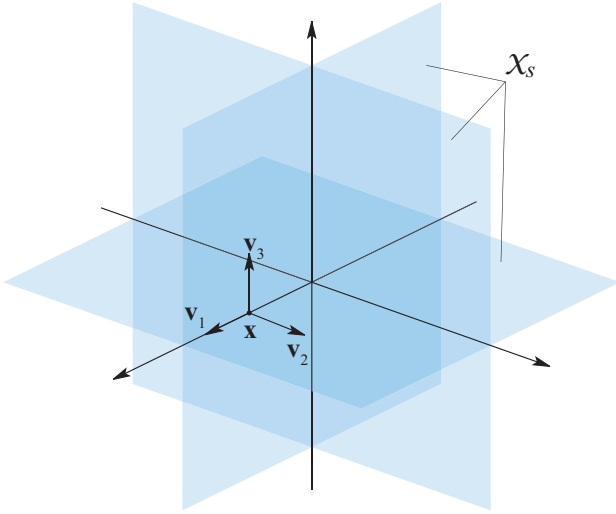
#### B. Further Analysis of the CCRB

In order to have a more profound understanding of the CCRB, we aim to compare it with a more intuitive quantity and analyze its asymptotic behavior. The following analysis will mainly focus on the maximal support case. As can be seen from (18) and (21), the CCRB of the two cases share a similar form, and thus the main results provided in the following text will still be valid for the nonmaximal support case with minor modifications.





(a) The maximal support case



(b) The nonmaximal support case

Fig. 1. A geometrical demonstration of the discontinuity between the neighborhood structures of the maximal and the nonmaximal support cases. The vectors  $\mathbf{v}_i$  are base vectors of the neighborhood subspace  $\mathcal{F}$ .

The expression (18) contains two terms, the first of which is rather simple, while the second of which is much more complicated. Fortunately, the following proposition relates the first term  $\sigma_{\mathbf{x}}^2 \text{tr}((\mathbf{A}_S^T \mathbf{A}_S)^{-1})$  to the MSE of the oracle pseudoinverse estimator, which provides an intuitive explanation. The definition and performance of the oracle pseudoinverse estimator can be summarized as follows.

**Proposition 2:** For a given support  $S$  whose size is  $s$ , define  $\hat{\mathbf{x}}_{\text{pinv}}$  to be the following estimator

$$\begin{aligned} (\hat{\mathbf{x}}_{\text{pinv}}(\mathbf{y}))_S &= \mathbf{A}_S^\dagger \mathbf{y} = (\mathbf{A}_S^T \mathbf{A}_S)^{-1} \mathbf{A}_S^T \mathbf{y}, \\ (\hat{\mathbf{x}}_{\text{pinv}}(\mathbf{y}))_{S^c} &= 0. \end{aligned} \quad (24)$$

This estimator is unbiased in the neighborhood of any parameter value whose support is  $S$ . The MSE of  $\hat{\mathbf{x}}_{\text{pinv}}$  is

$$\sigma_{\mathbf{x}}^2 \text{tr}((\mathbf{A}_S^T \mathbf{A}_S)^{-1}), \quad \forall \mathbf{x} : \text{supp}(\mathbf{x}) = S. \quad (25)$$

*Proof:* The proof is postponed to Appendix B.  $\square$

Proposition 2 demonstrates that the first term of the CCRB is just the MSE of the oracle pseudoinverse estimator. This term is also similar to the CCRB of the case where only measurement noise exists. Various references (e.g. [3], [20]) have shown that the CCRB when only measurement noise exists is the variance of the noise on  $\mathbf{y}$  multiplied by the trace of  $(\mathbf{A}_S^T \mathbf{A}_S)^{-1}$ , and the oracle pseudoinverse estimator achieves this bound.

The second term of (18) is more complicated. This term stems from the dependence of the variance of the total noise on the parameter  $\mathbf{x}$ , and it reveals a possibility that this term might help estimate  $\mathbf{x}$  more accurately. However, one still hopes that this term is not dominant in the CCRB, therefore we aim to bound this term by some simpler alternative, and especially to study how it varies versus the dimension of the signal.

In order to bound the second term, some assumptions have to be made on the matrix  $\mathbf{A}$ .

**Assumption 1:** For the sensing matrix  $\mathbf{A}$  in (18), it is assumed that there exist constants  $\vartheta_{l,s} \in (0, 1)$  and  $\vartheta_{u,s} > 0$  such that

$$(1 - \vartheta_{l,s}) \|\mathbf{x}\|_{\ell_2}^2 \leq \|\mathbf{A}\mathbf{x}\|_{\ell_2}^2 \leq (1 + \vartheta_{u,s}) \|\mathbf{x}\|_{\ell_2}^2 \quad (26)$$

for any  $s$ -sparse parameter  $\mathbf{x}$ . Because any constants that are greater than  $\vartheta_{l,s}$  or  $\vartheta_{u,s}$  respectively can still satisfy the above inequalities, in the following  $\vartheta_{l,s}$  and  $\vartheta_{u,s}$  are used to denote the smallest such constants.

**Remark 2:** This assumption is very similar to the commonly used restricted isometry property [34], [35], and possesses the same form as the asymmetric restricted isometry property proposed in [36]. However, the sensing matrix is not restricted to be underdetermined in the above assumption.

Assumption 1 actually bounds the eigenvalues of  $\mathbf{A}_S^T \mathbf{A}_S$  that appears in the second term of the CCRB. Armed with this assumption, the following theorem provides lower and upper bounds on the second term of the CCRB.

**Theorem 3:** Denote the opposite of the second term of the CCRB as  $d_{\text{CCRB}}$ , i.e.

$$d_{\text{CCRB}} = \sigma_{\mathbf{x}}^2 \cdot \frac{2m\sigma_e^4 \|(\mathbf{A}_S^T \mathbf{A}_S)^{-1} \mathbf{x}_S\|_{\ell_2}^2}{\sigma_{\mathbf{x}}^2 + 2m\sigma_e^4 \mathbf{x}_S^T (\mathbf{A}_S^T \mathbf{A}_S)^{-1} \mathbf{x}_S}. \quad (27)$$

Then  $d_{\text{CCRB}}$  satisfies the following inequalities:

$$\begin{aligned} d_{\text{CCRB}} &\leq \sigma_{\mathbf{x}}^2 \cdot \frac{(1 + \vartheta_{u,s})^2}{(1 - \vartheta_{l,s})^2} \\ &\quad \times \frac{2c_e}{2(1 - \vartheta_{l,s})c_e + 1 + \vartheta_{u,s} + c_n/c_e}, \end{aligned} \quad (28)$$

$$\begin{aligned} d_{\text{CCRB}} &\geq \sigma_{\mathbf{x}}^2 \cdot \frac{(1 - \vartheta_{l,s})^2}{(1 + \vartheta_{u,s})^2} \\ &\quad \times \frac{2c_e}{2(1 + \vartheta_{u,s})c_e + 1 - \vartheta_{l,s} + c_n/c_e}, \end{aligned} \quad (29)$$

where

$$\begin{aligned} c_e &= \frac{m\sigma_e^2}{\sum_{i=1}^m \sum_{j \in S} A_{ij}^2} = \frac{m\sigma_e^2}{\text{tr}(\mathbf{A}_S^T \mathbf{A}_S)}, \\ c_n &= \frac{m\sigma_n^2}{\|\mathbf{x}\|_{\ell_2}^2} \end{aligned}$$

indicate the matrix perturbation level and the measurement noise level<sup>2</sup> respectively. The ratio  $\gamma_{\text{CCRB}} = d_{\text{CCRB}}/(\text{CCRB} + d_{\text{CCRB}})$ , i.e. the ratio of the second term to the first term of the CCRB, is bounded by the following inequalities:

$$\gamma_{\text{CCRB}} \leq \frac{1}{s} \cdot \frac{(1 + \vartheta_{u,s})^3}{(1 - \vartheta_{l,s})^2} \times \frac{2c_e}{2(1 - \vartheta_{l,s})c_e + 1 + \vartheta_{u,s} + c_n/c_e} \quad (30)$$

$$\gamma_{\text{CCRB}} \geq \frac{1}{s} \cdot \frac{(1 - \vartheta_{l,s})^3}{(1 + \vartheta_{u,s})^2} \times \frac{2c_e}{2(1 + \vartheta_{u,s})c_e + 1 - \vartheta_{l,s} + c_n/c_e} \quad (31)$$

*Proof:* See Appendix C.  $\square$

Theorem 3 provides a very simple approximate expression that captures how  $d_{\text{CCRB}}$  and  $\gamma_{\text{CCRB}}$  vary with the noise level  $c_e$  and  $c_n$ :

$$d_{\text{CCRB}} \approx \sigma_{\mathbf{x}}^2 \cdot \frac{2c_e}{2c_e + 1 + c_n/c_e}, \quad (32)$$

$$\gamma_{\text{CCRB}} \approx \frac{1}{s} \cdot \frac{2c_e}{2c_e + 1 + c_n/c_e}, \quad (33)$$

provided that the constants  $\vartheta_{l,s}$  and  $\vartheta_{u,s}$  are small compared to 1. It is easily verified that the quantity  $2c_e/(2c_e + 1 + c_n/c_e)$  is always less than 1, and therefore the ratio  $\gamma_{\text{CCRB}}$  can be upper-bounded approximately as  $1/s$ . Furthermore, (33) implies that as  $s$  increases, the second term  $d_{\text{CCRB}}$  becomes less and less important, and finally becomes negligible. This can be considered as the asymptotic behavior of  $d_{\text{CCRB}}$  and the CCRB, which can be summarized as the following corollary.

*Corollary 1:* Assume that there exist constants  $\epsilon_l \in (0, 1)$  and  $\epsilon_u > 0$  such that when  $s$  tends to infinity, the constants  $\vartheta_{l,s}$  and  $\vartheta_{u,s}$  keep satisfying  $\vartheta_{l,s} < \epsilon_l$  and  $\vartheta_{u,s} < \epsilon_u$  for every  $s$ . Then if  $c_e$  and  $c_n$  remains constant, the ratio  $\gamma_{\text{CCRB}}$  possesses the following asymptotic behavior:

$$\frac{A}{s} \leq \gamma_{\text{CCRB}} \leq \frac{B}{s}, \quad (34)$$

where  $A$  and  $B$  are some positive constants.

*Remark 3:* This corollary demonstrates that as  $s \rightarrow \infty$ , the CCRB approaches  $\sigma_{\mathbf{x}}^2 \text{tr}((\mathbf{A}_S^T \mathbf{A}_S)^{-1})$ , while the latter is just the MSE of the oracle pseudoinverse estimator. The estimator is the solution of the following minimization problem:

$$\arg \min_{\mathbf{x}_S} \|\mathbf{y} - \mathbf{A}_S \mathbf{x}_S\|_{\ell_2}^2,$$

which merely minimizes the residual and totally ignores the fact that the noise is dependent on  $\mathbf{x}$ . Therefore it can be concluded that as  $s$  increases, less information can be possibly obtained from the dependence of the noise term on  $\mathbf{x}$  to help reduce the estimation error, and finally this dependence can be ignored.

<sup>2</sup>One may argue that  $m\sigma_n^2/\|\mathbf{A}\mathbf{x}\|_{\ell_2}^2$  seems more reasonable as an indication of the measurement noise level. However, because of Assumption 1, one has  $\|\mathbf{A}\mathbf{x}\|_{\ell_2}^2 \approx \|\mathbf{x}\|_{\ell_2}^2$ , and thus for simplicity  $m\sigma_n^2/\|\mathbf{x}\|_{\ell_2}^2$  is employed instead.

#### IV. THE HAMMERSLEY-CHAPMAN-ROBBINS BOUND

The constrained CRB given in the above section possesses a simple closed form, but it takes into account only the unbiasedness in the neighborhood of a specific parameter value rather than the global unbiasedness for all sparse vectors. Therefore it can be anticipated that for estimators that are globally unbiased for sparse parameter values (i.e. for all estimators in  $\mathcal{U}$ ), the CCRB is not a very tight lower bound.

In this section, the Hammersley-Chapman-Robbins bound (HCRB) is derived for sparse estimation under the setting of general perturbation. However, the calculation of the HCRB for general sensing matrix  $\mathbf{A}$  is much more complicated, and therefore attention is focussed only on the simplest case of unit sensing matrix in this section [27], [37]. Nevertheless, the HCRB of this simple case is still instructive for us to have a qualitative understanding of the HCRB for general cases.

The HCRB in the context of sparse estimation with general perturbation can be summarized as the following lemma.

*Lemma 2:* In the setting given in Section II, consider a specific parameter value  $\mathbf{x} \in \mathcal{X}_s$ . Suppose  $\{\mathbf{v}_i\}_{i=1}^k$  are  $k$  vectors such that  $\mathbf{x} + \mathbf{v}_i \in \mathcal{X}_s$  for all  $i = 1, \dots, k$ . Then the covariance matrix of any unbiased estimator  $\hat{\mathbf{x}} \in \mathcal{U}$  at  $\mathbf{x}$  satisfies

$$\text{Cov}(\hat{\mathbf{x}}) \succeq \mathbf{V} \mathbf{H}^\dagger \mathbf{V}^T. \quad (35)$$

Here the matrix  $\mathbf{V}$  is given by

$$\mathbf{V} = [\mathbf{v}_1, \dots, \mathbf{v}_k], \quad (36)$$

and the  $(i, j)$ th element of  $\mathbf{H}$  is

$$H_{ij} = \left( \frac{\sigma_{\mathbf{x}}^2 \varsigma_{\mathbf{x}, \mathbf{v}_i, \mathbf{v}_j}^2}{\sigma_{\mathbf{x}+\mathbf{v}_i}^2 \sigma_{\mathbf{x}+\mathbf{v}_j}^2} \right)^{\frac{m}{2}} \exp \left[ -\frac{\|\mathbf{A}\mathbf{v}_i\|_{\ell_2}^2}{2\sigma_{\mathbf{x}+\mathbf{v}_i}^2} - \frac{\|\mathbf{A}\mathbf{v}_j\|_{\ell_2}^2}{2\sigma_{\mathbf{x}+\mathbf{v}_j}^2} + \frac{\varsigma_{\mathbf{x}, \mathbf{v}_i, \mathbf{v}_j}^2}{2} \left\| \frac{\mathbf{A}\mathbf{v}_i}{\sigma_{\mathbf{x}+\mathbf{v}_i}^2} + \frac{\mathbf{A}\mathbf{v}_j}{\sigma_{\mathbf{x}+\mathbf{v}_j}^2} \right\|_{\ell_2}^2 \right] - 1, \quad (37)$$

where

$$\frac{1}{\varsigma_{\mathbf{x}, \mathbf{v}_i, \mathbf{v}_j}^2} = \frac{1}{\sigma_{\mathbf{x}+\mathbf{v}_i}^2} + \frac{1}{\sigma_{\mathbf{x}+\mathbf{v}_j}^2} - \frac{1}{\sigma_{\mathbf{x}}^2}. \quad (38)$$

*Proof:* The proof is postponed to Appendix D.  $\square$

It can be seen from Lemma 2 that the HCRB is actually a family of lower bounds of unbiased estimators. By employing different sets of  $\mathbf{v}_i$ , one will generally get different HCRBs, and the tightest one is their supremum. However, it is often impossible to obtain a closed-form expression of the supreme value of the HCRB family, and thus our task is to employ a certain set of  $\mathbf{v}_i$  in the hope that the corresponding HCRB will be simple and easy to analyze.

By appropriately choosing a set of  $\mathbf{v}_i$  and applying some special techniques, the following theorem of the HCRB<sup>3</sup> will be obtained.

*Theorem 4:* Assume that  $n \geq 2$ , and denote  $\beta = x_q^2/\sigma_{\mathbf{x}}^2$ , where  $x_q$  is the smallest entry in magnitude of the parameter

<sup>3</sup>This lower bound is actually a limit of a family of HCRBs. Nevertheless this bound will still be referred to as the HCRB in the following text.

$\mathbf{x}$ , with  $q$  the corresponding index. Then the MSE of any estimator  $\hat{\mathbf{x}} \in \mathcal{U}$  satisfies

$$\begin{aligned} & \text{mse}(\hat{\mathbf{x}}) \\ & \geq \sigma_{\mathbf{x}}^2 \left( s - \frac{2n\sigma_e^4 \|\mathbf{x}\|_{\ell_2}^2}{\sigma_{\mathbf{x}}^2 + 2n\sigma_e^4 \|\mathbf{x}\|_{\ell_2}^2} \right) + \frac{\sigma_{\mathbf{x}}^2(n-s)\beta \exp(-\beta)}{\exp \beta - 1} \\ & \quad \times \left( 1 - \frac{1}{n-s + \exp \beta \cdot (1-g(\beta))^{-1}} \right) \end{aligned} \quad (39)$$

for any  $\mathbf{x} \in \mathcal{X}_s$  with  $\|\mathbf{x}\|_{\ell_0} = s$ . The specific form of the function  $g(\beta)$  is

$$g(\beta) = \frac{\beta(1-2\sigma_e^2\beta)^2}{(\exp \beta - 1)(1+2n\sigma_e^4\beta)}, \quad (40)$$

and  $g(\beta)$  satisfies

$$0 \leq g(\beta) < 1, \quad \forall \beta > 0, n \geq 2. \quad (41)$$

When  $\sigma_n$  and  $\sigma_e$  are fixed, ones has

$$\lim_{x_q \rightarrow 0} g(\beta) = 1. \quad (42)$$

*Proof:* See Appendix E.  $\square$

The quantity  $\beta = x_q^2/\sigma_{\mathbf{x}}^2$  represents a special kind of signal-to-noise ratio, and can be named the ‘‘worst case entry SNR’’ [27]. This quantity plays a central role in the transition from maximal support to nonmaximal support. However, it should be noticed that there exists an upper bound of the domain of  $\beta$  if  $\sigma_e \neq 0$ :

$$\begin{aligned} \beta &= \frac{x_q^2}{\sigma_n^2 + \sigma_e^2 \|\mathbf{x}\|_{\ell_2}^2} \leq \frac{x_q^2}{\sigma_e^2 \|\mathbf{x}\|_{\ell_2}^2} \\ &= \frac{1}{\sigma_e^2 \sum x_i^2/x_q^2} \leq \frac{1}{s\sigma_e^2}. \end{aligned} \quad (43)$$

Therefore the situation here is more complicated than that with only the measurement noise. One of the consequences is that when  $x_q \rightarrow +\infty$ , the HCRB does not generally tends to the CCRB of maximal support unless  $\sigma_e = 0$ , i.e.

$$\lim_{x_q \rightarrow +\infty} \frac{\text{HCRB} - \text{CCRB}_{\max \text{ supp}}}{\text{CCRB}_{\max \text{ supp}}} > 0, \quad \text{if } \sigma_e \neq 0. \quad (44)$$

This phenomenon reveals that the global unbiasedness has an essential effect on the problem of the  $\sigma_e \neq 0$  case. Fortunately, when  $\sigma_n$  and  $\sigma_e$  remains constant, the HCRB will converge to the CCRB of nonmaximal support as  $x_q \rightarrow 0$ , as can be seen from

$$\lim_{x_q \rightarrow 0} \text{HCRB} = \sigma_{\mathbf{x}}^2 \left( n - \frac{2n\sigma_e^4 \|\mathbf{x}\|_{\ell_2}^2}{\sigma_{\mathbf{x}}^2 + 2n\sigma_e^4 \|\mathbf{x}\|_{\ell_2}^2} \right). \quad (45)$$

Therefore it can be said that the gap between the maximal and nonmaximal cases is eliminated.

We compare the above result with other similar results appeared in literatures. In [27], a closed-form expression of the HCRB for the  $\sigma_e^2 = 0$  case is derived in a similar approach but with different choice of  $\{\mathbf{v}_i\}$ . Their closed-form result is tighter than ours when  $\beta$  is sufficiently large, but is not as tight as ours in the low  $\beta$  range and fails to close the gap between maximal and nonmaximal cases. In [37], another lower bound is provided and is tighter than ours for all  $\beta > 0$ , but their

derivation is based on the RKHS formulation of the Barankin bound which is difficult to be generalized to the  $\sigma_e^2 \neq 0$  case. Despite the fact that our bound is not the tightest, it still provides a correct qualitative trend of the lower bound of sparse estimation, and is able to deal with matrix perturbation without much effort.

#### A. Further Analysis of the HCRB

It has already been mentioned that the domain of  $\beta$  possesses an upper bound which is not greater than  $1/s\sigma_e^2$ , and thus the  $x_q \rightarrow +\infty$  limit of the HCRB does not coincide with the CCRB. This difference implicates the effect of the matrix perturbation on the HCRB and is the major topic of this subsection. For simplicity of analysis, in the following text it is assumed that as  $x_q \rightarrow +\infty$ , all other components of  $\mathbf{x}$  equal  $x_q$  asymptotically, which leads to the fact that the upper bound of  $\beta$  is  $1/s\sigma_e^2$ .

As  $x_q \rightarrow +\infty$ , the HCRB asymptotically equals

$$\begin{aligned} & \sigma_{\mathbf{x}}^2 \left( s - \frac{2n\sigma_e^4 \|\mathbf{x}\|_{\ell_2}^2}{\sigma_{\mathbf{x}}^2 + 2n\sigma_e^4 \|\mathbf{x}\|_{\ell_2}^2} \right) + \frac{\sigma_{\mathbf{x}}^2(n-s) \exp(-1/s\sigma_e^2)}{s\sigma_e^2(\exp(1/s\sigma_e^2) - 1)} \\ & \quad \times \left( 1 - \frac{1}{n-s + \exp(1/s\sigma_e^2)(1-g(1/s\sigma_e^2))^{-1}} \right). \end{aligned}$$

The above expression contains two terms, the first of which is just the CCRB of the maximal support case. For the second term, it can be seen that the  $\sigma_e$ 's mainly appear in the exponentials, which demonstrates that there exists a particular value of  $\sigma_e$  that separates the low  $\sigma_e$  region and the high  $\sigma_e$  region. This particular value will be named the transition value of  $\sigma_e$  and will be denoted by  $\sigma_{e,t}$ .

The analysis and computation of  $\sigma_{e,t}$  is simple. When  $\sigma_e^2 \ll 1/s$ , one has  $\exp(1/s\sigma_e^2) \gg 1$  and  $\exp(-1/s\sigma_e^2) \approx 0$ , and thus the HCRB approximates

$$\sigma_{\mathbf{x}}^2 \left( s - \frac{2n\sigma_e^4 \|\mathbf{x}\|_{\ell_2}^2}{\sigma_{\mathbf{x}}^2 + 2n\sigma_e^4 \|\mathbf{x}\|_{\ell_2}^2} \right),$$

which is just the maximal support CCRB. However, if the matrix perturbation is large enough so that  $\sigma_e^2 \gg 1/s$ , the difference between the HCRB and CCRB cannot be neglected. Therefore  $1/\sqrt{s}$  can be regarded as the transition point  $\sigma_{e,t}$ : when  $\sigma_e < \sigma_{e,t}$ , the HCRB degenerates to the CCRB as  $x_q \rightarrow +\infty$ ; when  $\sigma_e > \sigma_{e,t}$ , the lower bound is raised for large  $x_q$  and does not degenerate to the CCRB.

The theory of the transition point  $\sigma_{e,t}$  may have a geometrical explanation which is not rigorous but very intuitive. The set  $\mathcal{X}_s$  can be regarded as the union of  $s$ -dimensional hyperplanes spanned by  $s$  coordinate axes respectively. The sparse parameter  $\mathbf{x}$  lies on one of the hyperplanes  $\Sigma_s$  and is surrounded by a noise ball whose radius is  $r^2 = \sigma_{\mathbf{x}}^2$ . As  $x_q \rightarrow +\infty$ , the radius satisfies  $r^2 \sim \sigma_e^2 \|\mathbf{x}\|_{\ell_2}^2 \sim s\sigma_e^2 x_q$ . The transition point corresponds to the tangency of the noise ball to one of the hyperplanes of  $\mathcal{X}_s$  apart from  $\Sigma_s$ , and the high and low  $\sigma_e$  regimes correspond to whether or not the noise ball intersects with another hyperplane (See Fig. 2). It can be easily verified that this geometrical interpretation gives out correct value of the transition point  $\sigma_{e,t}$ .

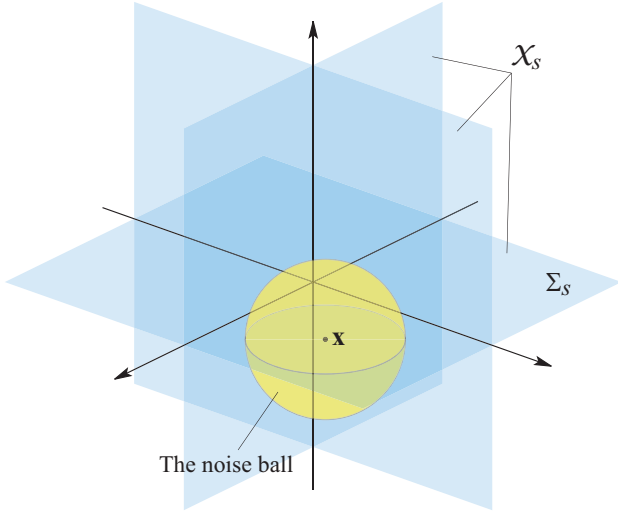


Fig. 2. The geometrical interpretation of the transition point  $\sigma_{e,t}$ . The hyperplanes are part of the set  $\mathcal{X}_s$ , and the sparse parameter  $\mathbf{x}$  lies on  $\Sigma_s$ . The radius of the noise ball is  $r^2 \sim s\sigma_e^2 x_q$ . If this ball intersects another hyperplane, such situation belongs to the high  $\sigma_e$  regime; otherwise it belongs to the low  $\sigma_e$  regime. For the low  $\sigma_e$  regime, the HCRB equals the corresponding CCRB approximately if  $x_q$  is sufficiently large; for the high  $\sigma_e$  regime, the HCRB is evidently higher than the corresponding CCRB.

## V. NUMERICAL RESULTS

In this section, numerical simulations are performed in order to substantiate the theoretical results presented in the previous sections.

### A. Numerical Analysis of $\gamma_{\text{CCRB}}$

Numerical experiments are first made on the CCRB, or equivalently, on the quantity  $\gamma_{\text{CCRB}}$ . We wish to verify that the formula (33) is valid and can demonstrate how  $\gamma_{\text{CCRB}}$  varies versus the perturbation level  $c_e$  and the noise level  $c_n$ . Before we perform the numerical simulations, it is worthwhile to analyze the formula (33) first with the help of its graph obtained by numerical approaches.

Define the function in the approximate formula (33)

$$\gamma(c_e, c_n) = \frac{1}{s} \frac{2c_e}{2c_e + 1 + c_n/c_e}. \quad (46)$$

The graphs of the approximate function  $\gamma(c_e, c_n)$  with varying  $c_e$  and  $c_n$  are shown in Fig. 3. It can be seen that when  $c_n$  is fixed, the function  $\gamma(c_e, c_n)$  is monotonically increasing of  $c_e$ , with limits  $\gamma(0^+, c_n) = 0$  and  $\gamma(+\infty, c_n) = 1/s$ . It can also be seen that for each fixed  $c_n$ , there exists a transition point  $c_{e,t}$  of the curve which approximately separates the high  $c_e$  regime and low  $c_e$  regime: when  $c_e \ll c_{e,t}$ , one has  $\gamma(c_e, c_n) \approx 0$ , while for  $c_e \gg c_{e,t}$ , one has  $\gamma(c_e, c_n) \approx 1/s$ . This transition point can be defined as the point such that  $\gamma(c_{e,t}, c_n) = 1/2s$ . For the special case  $c_n = 0$ , the transition point is  $c_{e,t} = 1/2 = -3$  dB; for general  $c_n > 0$ ,  $c_{e,t}$  is the positive root of the quadratic function  $2x^2 - x - c_n = 0$ .

When  $c_e$  is fixed, the function  $\gamma(c_e, c_n)$  is monotonically decreasing of  $c_n$ . Fig. 3 also indicates that the transition point  $c_{e,t}(c_n)$  is a monotonically increasing function of  $c_n$ , which is a direct corollary of the monotonicity of  $\gamma(c_e, c_n)$  with respect to  $c_n$ .

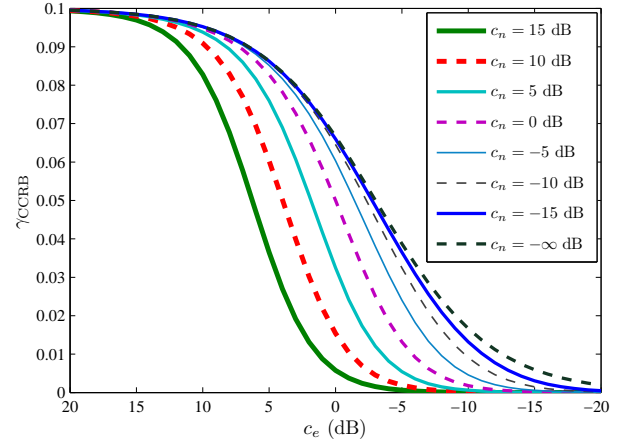


Fig. 3. The graphs of the approximate formula of  $\gamma_{\text{CCRB}}$  as a function of  $c_e$  with different settings of  $c_n$ . The theoretical approximate formula is given by (33).

In order to verify that the general trend of  $\gamma_{\text{CCRB}}$  can be described by the function  $\gamma(c_e, c_n)$ , numerical results of the quantity  $\gamma_{\text{CCRB}}$  are simulated. The relation of the size of the sensing matrix  $\mathbf{A}$  and the sparsity of  $\mathbf{x}$  is set to be  $n = 20s, m = 10s$ , and  $s = 10$ . The perturbation level  $c_e$  varies from 20 dB to -20 dB, and the noise level  $c_n$  is set to be 0, -5 dB, and 15 dB respectively. The entries of  $\mathbf{A}$  are drawn from i.i.d. standard normal distribution  $\mathcal{N}(0, 1/m)$ . Such generation of  $\mathbf{A}$  is standard in the field of compressive sensing, and ensures the existence of the constants  $\vartheta_{l,s}$  and  $\vartheta_{u,s}$  with overwhelming probability [35], [36]. For the parameter  $\mathbf{x}$ , the support is equiprobably chosen from all subsets of  $\{1, \dots, n\}$  with size  $s$ , and the nonzero entries satisfy i.i.d. Bernoulli-type distribution with  $P(x_k = -1) = P(x_k = 1) = 1/2, k \in \text{supp}(\mathbf{x})$ . Each simulation runs 30 times so that 30 different groups of  $\mathbf{A}$  and  $\mathbf{x}$  are tested.

The results of these simulations are shown in Fig. 4. Those points which are marked by “x” are raw numerical simulation results, and the solid lines in these figures are graphs of the approximate function  $\gamma(c_e, c_n)$ . It can be seen from the simulation results that the curves of the function  $\gamma(c_e, c_n)$  can correctly describe how  $\gamma_{\text{CCRB}}$  varies versus  $c_e$  and  $c_n$ . These figures also demonstrate that the solid curves lie almost in the middle of the raw data points, which partially justifies the validity of the approximate formula and the bounds given by (28) and (29).

Next we wish to verify the asymptotic behavior of  $\gamma_{\text{CCRB}}$ , i.e. the  $s^{-1}$  law given by Corollary 1. This time the sparsity  $s$  varies from 3 to 300 with exponentially increasing increments, but  $n$  and  $m$  are still set to be  $n = 20s$  and  $m = 10s$ . The generations of  $\mathbf{A}$  and  $\mathbf{x}$  are the same as in previous simulations. Previous literatures have verified theoretically and experimentally that such setting of  $\mathbf{A}$  can ensure the existence of the constants  $\epsilon_l$  and  $\epsilon_u$  with high probability [36]. For the perturbation and noise level, nine groups of values are employed.

The results are illustrated in Fig. 5. The dotted points are raw experimental data of  $\gamma_{\text{CCRB}}$ , and the solid straight line



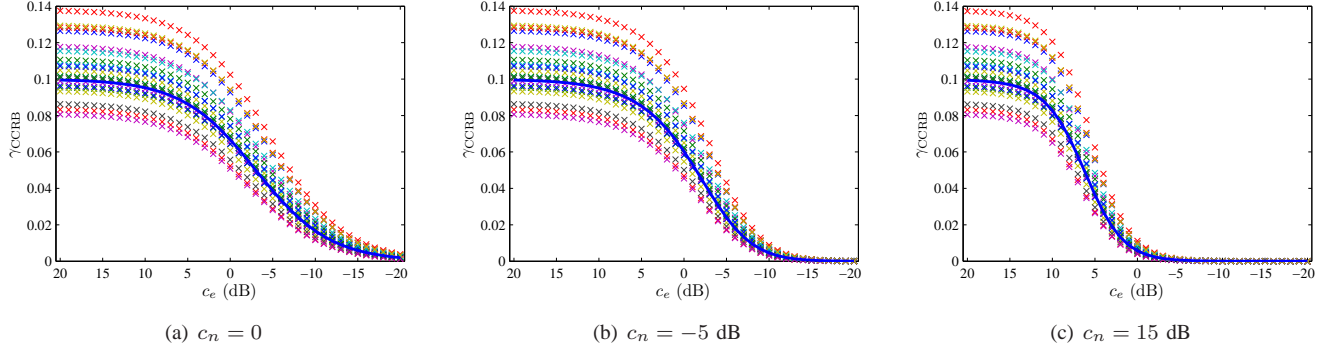


Fig. 4.  $\gamma_{\text{CRLB}}$  as a function of  $c_e$  with different settings of  $c_n$ . Data points marked by “x” are generated by simulation results. The solid lines represent the corresponding values calculated by the approximate expression (33).

is the  $s^{-1}$  line calculated by the approximate formula (33). Notice that we have employed the log-log scaling of the coordinate system so that the  $s^{-1}$  law is represented by a straight line with slope  $-1$  in the graph, which makes it convenient to justify the theoretical results. It can be seen from the graphs that the data points can be upper and lower bounded by two  $s^{-1}$  curves, and that they cluster near the straight line given by the approximate formula (33). Therefore it can be concluded that the trend of  $\gamma_{\text{CRLB}}$  with respect to  $s$  can be described by the  $s^{-1}$  law.

### B. Numerical Analysis of the HCRB

Theoretical result of the unit sensing matrix is given by Theorem 4. It suggests a continuous transition from the maximal support case to the nonmaximal support case and is fairly easy to compute. On the other hand, the demand of a closed-form expression compromises potential tightness. Generally more testing points  $\mathbf{x} + \mathbf{v}_i$  will lead to tighter lower bounds which, however, will not possess simple closed-forms and can only be evaluated by numerical methods. Therefore we will simulate the lower bound given by Theorem 4 as well as lower bounds computed numerically with more testing points.

Before running the simulations, we first have a brief review of Theorem 4. It can be seen that the lower bound given by (39) consists of two parts: the maximal support CCRB and the additional term which connects the CCRB gap. Emphasis of numerical experiments will mainly be put on the additional term, and the common factor  $\sigma_x^2$  will be ignored. In other words, our analysis will be focussed on the following quantity:

$$d_{\text{HCRB}} = \frac{(n-s)\beta \exp(-\beta)}{\exp \beta - 1} \left( 1 - \frac{1}{n-s + \exp \beta (1-g(\beta))^{-1}} \right). \quad (47)$$

Detailed settings of the numerical simulations are as follows. For simplicity and convenience of analysis, the dimensions are  $n = m = 10s$ . The parameter  $\mathbf{x}$  is set to be  $[x_q, \dots, x_q, 0, \dots, 0]^T$ . Different settings of  $\sigma_e$  and  $\sigma_n$  are employed, and for each group of  $\{\sigma_e, \sigma_n\}$  we simulated the HCRB with varying  $x_q$  to get a graph of the quantity  $d_{\text{HCRB}}$ .

As mentioned in Subsection IV-A, there exists a transition point  $\sigma_{e,t}$  which separates the high and low  $\sigma_e$  regime. The

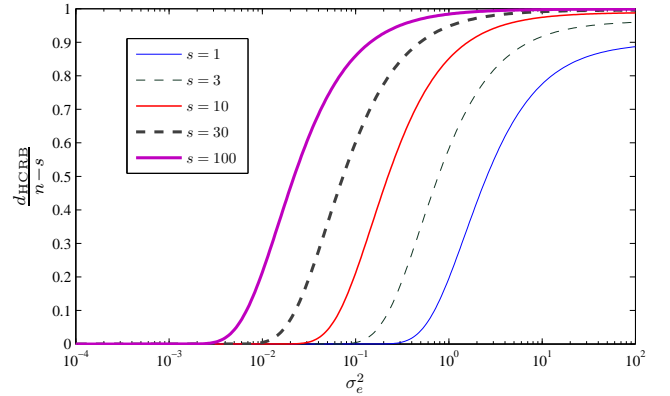


Fig. 6.  $d_{\text{HCRB}}/(n-s)$  versus  $\sigma_e$  with different settings of  $s$ .

first task is to verify the theory of transition point presented previously. The sparsities are set to be 1, 3, 10, 30 and 100 respectively, and for each setting of the sparsity,  $\sigma_e^2$  ranges from 0.0001 to 100. The measurement noise  $\sigma_n$  is set to be 0.1, and the HCRB for  $x_q = 1000$  is computed as a good approximation for the  $x_q \rightarrow +\infty$  case.

The numerical results are shown in Fig. 6, where  $d_{\text{HCRB}}$  is “normalized” by  $n-s$  so that the curves share a similar scale. It can be seen from the figure that the transition point for each  $s$  exists and can be well evaluated by  $\sigma_{e,t}^2 = 1/s$ . For  $\sigma_e \ll \sigma_{e,t}$ ,  $d_{\text{HCRB}}/(n-s)$  is much less than 1, and as  $\sigma_e \rightarrow 0$ ,  $d_{\text{HCRB}}/(n-s)$  tends to zero rapidly; for  $\sigma_e > \sigma_{e,t}$ ,  $d_{\text{HCRB}}/(n-s)$  cannot be neglected, and as  $\sigma_e \rightarrow +\infty$ ,  $d_{\text{HCRB}}/(n-s)$  possesses a limit which is of order 1.

Next we fix  $\sigma_e$  and  $\sigma_n$ , and test how  $d_{\text{HCRB}}$  varies versus  $x_q$ . The sparsity  $s$  is set to 1 for simplicity. Results are shown in Fig. 7. Fig. 7(a) corresponds to the situation where  $\sigma_n = 0.1$  is fixed with different  $\sigma_e$ ’s. It can be seen from the figure that when  $\sigma_e$  belongs to the low value regime (i.e.  $\sigma_e \ll \sigma_{e,t}$ , where  $\sigma_{e,t} = 1$  here), its effect on  $d_{\text{HCRB}}$  can be neglected. Moreover, each curve can be separated into three regions: the low  $x_q$  region where  $\text{HCRB} \approx \text{CCRB}_{\text{nonmax supp}}$ , the high  $x_q$  region where  $\text{HCRB} \approx \text{CCRB}_{\text{max supp}}$ , and the transition region which connects the low and high  $x_q$  region. However, when  $\sigma_e$  exceeds  $\sigma_{e,t}$ , the behavior of  $d_{\text{HCRB}}$  will become rather different and exhibits a more complex pattern.

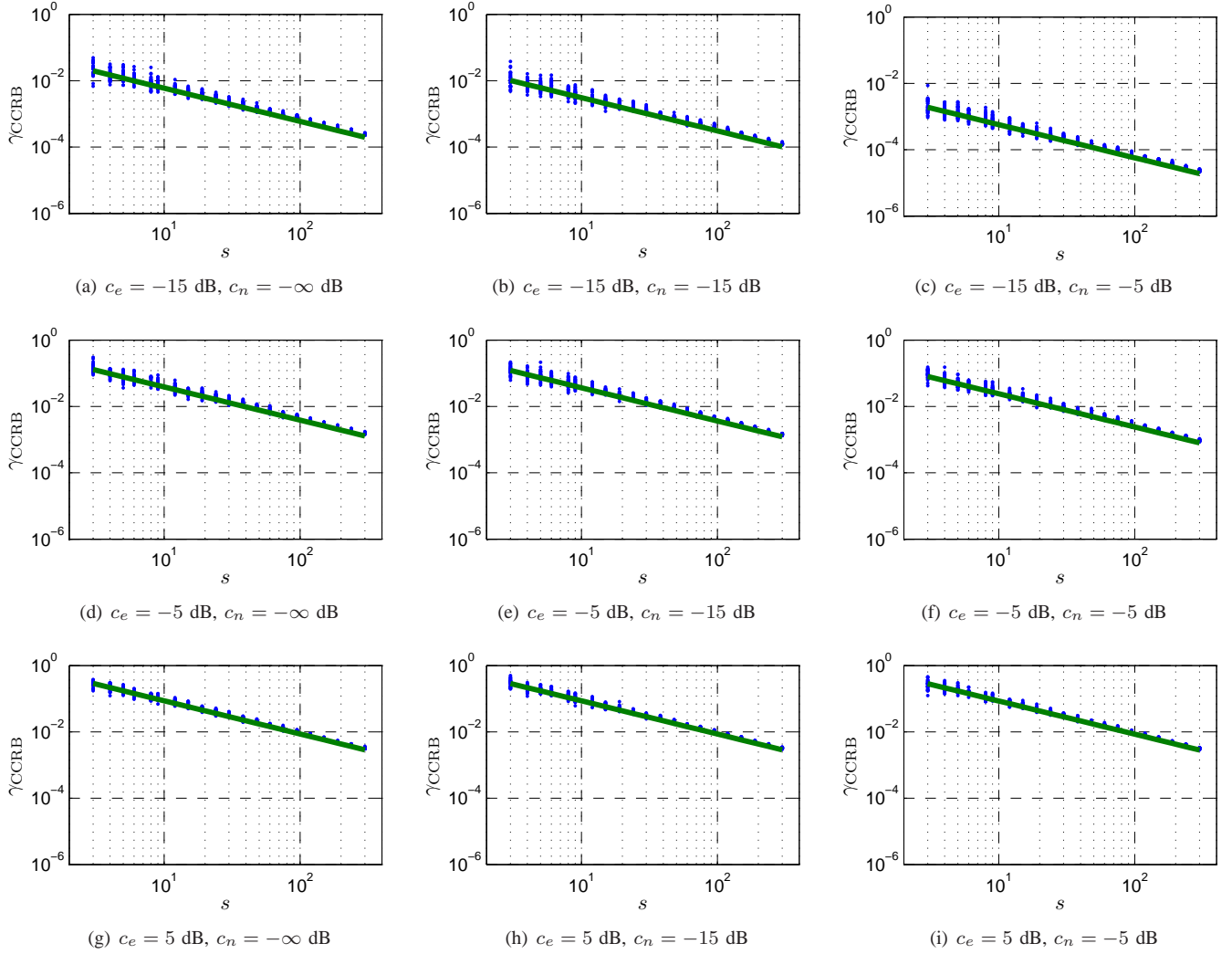


Fig. 5. Simulation results of  $\gamma_{\text{CRLB}}$  versus the support size  $s$  under different settings of  $c_e$  and  $c_n$ . Dotted data points are generated by numerical simulations, and the solid straight lines are computed by (33). Notice that the log-log scaling of the coordinate system makes the graph of  $s^{-1}$  a straight line of slope  $-1$ .

These phenomena demonstrate the way matrix perturbation influences the HCRB.

Fig. 7(b) corresponds to the situation where  $\sigma_e = 1$  is fixed with different  $\sigma_n$ 's. When  $\sigma_n = 0$ , it can be seen that  $d_{\text{HCRB}}$  remains constant because  $\beta = 1/\sigma_e^2$  in this case<sup>4</sup>. When  $\sigma_n \neq 0$ , it can be seen from the figure that the curves are translations of each other. This can be explained by the expression of  $\beta$  that  $\beta = x_q^2/(\sigma_n^2 + \sigma_e^2 x_q^2)$ , in which a multiple of  $\sigma_n$  is equivalent to a multiple of  $x_q$ . When  $s \geq 2$ , the curves will generally not be translations of each other, and the behavior with varying  $\sigma_n$  will be more complex. Nevertheless, the limits  $d_{\text{HCRB}}|_{x_q \rightarrow 0}$  and  $d_{\text{HCRB}}|_{x_q \rightarrow \infty}$  will be the same for all  $\sigma_n$ .

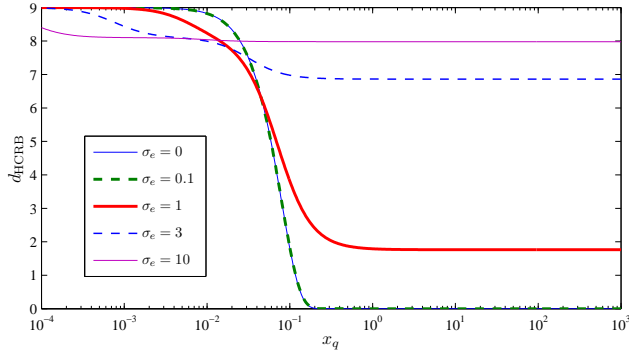
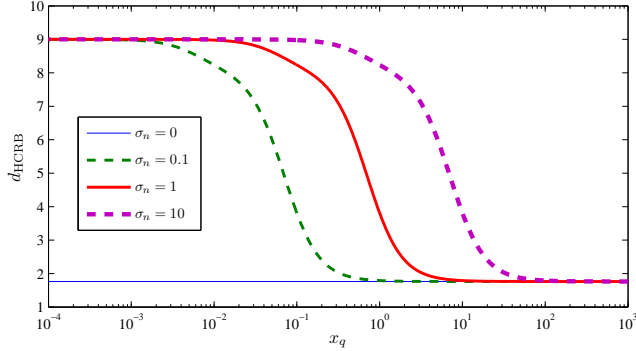
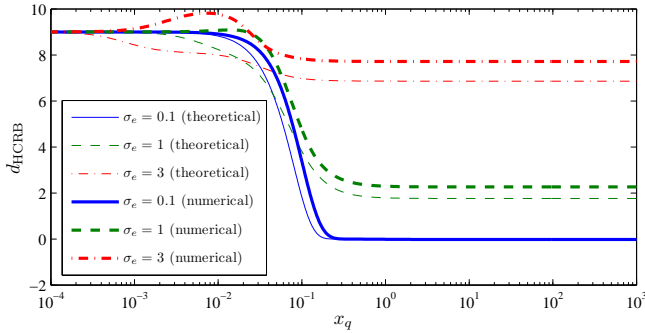
As mentioned before, more testing points of the HCRB will generally lead to a tighter lower bound, and thus we also compute the HCRB numerically with the following set of testing points in order to get a tighter bound as well as to

compare it with the theoretical result:

$$\begin{aligned} \{\mathbf{v}_i\} &= \mathcal{V}_{\text{supp}} \cup \mathcal{V}_{\text{nonsupp}}, \\ \mathcal{V}_{\text{supp}} &= \{0.01x_i \mathbf{e}_i : i \in S\} \cup \{-x_i \mathbf{e}_i : i \in S\}, \\ \mathcal{V}_{\text{nonsupp}} &= \{0.01x_i \mathbf{e}_i - x_k \mathbf{e}_k : i \notin S, k \in S\} \\ &\quad \cup \{x_i \mathbf{e}_i - x_k \mathbf{e}_k : i \notin S, k \in S\}, \end{aligned} \quad (48)$$

where  $S$  is the support of  $\mathbf{x}$ . The settings of parameter  $\mathbf{x}$  are the same as the previous experiment. The results are shown in Fig. 8 where the three typical cases  $\{\sigma_n = 0.1, \sigma_e = 0.1\}$ ,  $\{\sigma_n = 0.1, \sigma_e = 1\}$  and  $\{\sigma_n = 0.1, \sigma_e = 3\}$  are tested. It can be seen that when  $\sigma_e$  is below  $\sigma_{e,t}$ , the theoretical bound given by Theorem 4 is rather close to the numerical bound; the major different lies in the transition region of  $x_q$ , where the theoretical bound is slightly less than the numerical one. On the other hand, when  $\sigma_e$  is above  $\sigma_{e,t}$ , the numerical bound is not only larger than the theoretical one but also exhibits a rather complicated behavior. These behaviors of the HCRB reveal the complexity of the sensing matrix perturbation situation.

<sup>4</sup>When  $s \geq 2$ , however,  $d_{\text{HCRB}}$  will generally not remain constant as  $x_q$  varies.

(a)  $\sigma_n = 0.1$  with varying  $\sigma_e$ (b)  $\sigma_e = 1$  with varying  $\sigma_n$ Fig. 7.  $d_{\text{HCRB}}$  versus  $x_q$  with different settings of  $c_e$  and  $c_n$ .Fig. 8. Theoretical and numerical values of  $d_{\text{HCRB}}$ . The measurement noise variance is  $\sigma_n = 0.1$ . In the numerical case,  $d_{\text{HCRB}}$  is defined as  $(\text{HCRB} - \text{CCRB}_{\text{max supp}})/\sigma_{\mathbf{x}}^2$ .

## VI. CONCLUSION

In this paper, the performance bound of sparse estimation with general perturbation has been studied. Two widely-used types of lower bounds, the CCRB and the HCRB, have been calculated and analyzed. For the CCRB, we have derived its closed-form expression and analyzed its behavior. It has been shown that the CCRB is more complicated if there exists sensing matrix perturbation, but the additional term can be bounded and relatively tends to zero if the sensing matrix satisfies RIP-type conditions. For the HCRB, only the special case with unit sensing matrix is studied due to the complexity of calculation, but the results are still instructive

in that they are easy to analyze and can provide qualitative comprehension. It has been shown that the HCRB provides a tighter lower bound than the CCRB, and that it exhibits a satisfying transition behavior when the smallest entry of the parameter tends to zero. Numerical simulations have also been performed to substantiate these theoretical results as well as to give a more quantitative understanding of the theorems and formulas.

There are several future directions to be explored. First, the HCRB is obtained only for the unit sensing matrix case, which is useful for a qualitative comprehension but has apparent limitation. In many cases the sensing matrix cannot be assumed unit, and a more precise quantitative study on the performance bound also requires generalizing the HCRB to the general sensing matrix case. There may be two practical approaches to this problem. One is to derive a closed-form lower bound which is convenient to analyze and understand; the other is to find a tractable way to numerically compute the lower bound. However, both ways need further research and are still waiting for useful results.

Second, the HCRB provides a lower bound for globally unbiased estimators. However, recovery algorithms are quite likely to be biased in the sparse setting, and the bias is usually dependent on the noise variance. Moreover, there are occasions that biased estimators can achieve a lower MSE than unbiased estimators [38]. These problems also point out a possible direction for future study.

## APPENDIX A PROOF OF LEMMA 1

We first compute the likelihood function  $p(\mathbf{y}; \mathbf{x})$ . Notice that the problem (2) can be re-formulated as

$$\begin{aligned} \mathbf{y} &= \mathbf{A}\mathbf{x} + \mathbf{E}\mathbf{x} + \mathbf{n}, \\ &= \mathbf{A}\mathbf{x} + \mathbf{n}_{\mathbf{x}}, \end{aligned} \quad (49)$$

where  $\mathbf{n}_{\mathbf{x}} = \mathbf{E}\mathbf{x} + \mathbf{n}$  denotes the equivalent noise. Apparently (1) and (49) share a similar formulation, which hints a close relation between the two conditions of noisy observation and general perturbation.

Let us first find the probability distribution of  $\mathbf{E}\mathbf{x}$ . Because the elements of  $\mathbf{E}$  are drawn i.i.d. from Gaussian distribution, it is well-known from elementary probability theory that  $\mathbf{E}\mathbf{x}$  is an  $m$ -dimensional Gaussian-distributed random vector. It can also be seen that  $\mathbf{E}\mathbf{x}$  is independent of  $\mathbf{n}$ .

Denoting the  $(i, j)$ th element of  $\mathbf{E}$  as  $e_{ij}$  and  $k$ th element of  $\mathbf{x}$  as  $x_k$ , the  $i$ th component of  $\mathbf{E}\mathbf{x}$  can be formulated as

$$(\mathbf{E}\mathbf{x})_i = \sum_{k=1}^n e_{ik}x_k, \quad (50)$$

from which it is obviously seen that  $E[\mathbf{E}\mathbf{x}] = \mathbf{0}$ . The covariance of  $(\mathbf{E}\mathbf{x})_i$  and  $(\mathbf{E}\mathbf{x})_j$  is given by

$$\begin{aligned} \text{Cov}((\mathbf{E}\mathbf{x})_i, (\mathbf{E}\mathbf{x})_j) &= E[(\mathbf{E}\mathbf{x})_i(\mathbf{E}\mathbf{x})_j] \\ &= E\left[\sum_{k,l=1}^n e_{ik}e_{jl}x_kx_l\right] = \sum_{k,l=1}^n x_kx_l E[e_{ik}e_{jl}] \\ &= \sum_{k,l=1}^n x_kx_l \sigma_e^2 \delta_{ij} \delta_{kl} = \sigma_e^2 \|\mathbf{x}\|_{\ell_2}^2 \delta_{ij}, \end{aligned} \quad (51)$$

where  $\delta_{ij}$  is the Kronecker delta. Thus the covariance matrix of  $\mathbf{Ex}$  is

$$\text{Cov}(\mathbf{Ex}) = \sigma_e^2 \|\mathbf{x}\|_{\ell_2}^2 \mathbf{U}_m. \quad (52)$$

The above result shows that the additive noises  $\mathbf{Ex}$  can be viewed as i.i.d. Gaussian noises with variance  $\sigma_e^2 \|\mathbf{x}\|_{\ell_2}^2$ .

Given the probability distribution of  $\mathbf{Ex}$ , it can be derived from the mutual independence of  $\mathbf{Ex}$  and  $\mathbf{n}$  that the total noise term  $\mathbf{n}_x = \mathbf{Ex} + \mathbf{n}$  satisfies the distribution  $\mathcal{N}(0, (\sigma_e^2 \|\mathbf{x}\|_{\ell_2}^2 + \sigma_n^2) \mathbf{U}_m)$ . Therefore the likelihood function is given by

$$L(\mathbf{x}) = \frac{1}{(2\pi\sigma_x^2)^{\frac{m}{2}}} \exp \left[ -\frac{(\mathbf{y} - \mathbf{Ax})^T (\mathbf{y} - \mathbf{Ax})}{2\sigma_x^2} \right], \quad (53)$$

where

$$\sigma_x^2 = \sigma_e^2 \|\mathbf{x}\|_{\ell_2}^2 + \sigma_n^2. \quad (54)$$

Next we compute the FIM with the help of the likelihood function. The gradient of the log likelihood function  $\ln p(\mathbf{y}; \mathbf{x})$  is given by

$$\begin{aligned} \nabla_{\mathbf{x}} \ln p(\mathbf{y}; \mathbf{x}) &= \frac{1}{\sigma_e^2 \mathbf{x}^T \mathbf{x} + \sigma_n^2} \left[ \mathbf{A}^T (\mathbf{y} - \mathbf{Ax}) \right. \\ &\quad \left. + \frac{\|\mathbf{y} - \mathbf{Ax}\|_{\ell_2}^2 \mathbf{x}}{\sigma_e^2 \mathbf{x}^T \mathbf{x} + \sigma_n^2} \right] - m \frac{\sigma_e^2 \mathbf{x}}{\sigma_e^2 \mathbf{x}^T \mathbf{x} + \sigma_n^2}, \end{aligned} \quad (55)$$

and therefore

$$\begin{aligned} &(\nabla_{\mathbf{x}} \ln p(\mathbf{y}; \mathbf{x})) (\nabla_{\mathbf{x}}^T \ln p(\mathbf{y}; \mathbf{x})) \\ &= \frac{m^2 \sigma_e^4}{(\sigma_e^2 \mathbf{x}^T \mathbf{x} + \sigma_n^2)^2} \mathbf{xx}^T - \frac{2m\sigma_e^4 \|\mathbf{y} - \mathbf{Ax}\|_{\ell_2}^2}{(\sigma_e^2 \mathbf{x}^T \mathbf{x} + \sigma_n^2)^3} \mathbf{xx}^T \\ &\quad + \frac{1}{(\sigma_e^2 \mathbf{x}^T \mathbf{x} + \sigma_n^2)^2} \mathbf{A}^T (\mathbf{y} - \mathbf{Ax}) (\mathbf{y} - \mathbf{Ax})^T \mathbf{A} \\ &\quad + \frac{\sigma_e^4 \|\mathbf{y} - \mathbf{Ax}\|_{\ell_2}^4}{(\sigma_e^2 \mathbf{x}^T \mathbf{x} + \sigma_n^2)^4} \mathbf{xx}^T + \text{terms linear in } (\mathbf{y} - \mathbf{Ax}) \\ &\quad + \text{terms cubic in } (\mathbf{y} - \mathbf{Ax}). \end{aligned} \quad (56)$$

The specific forms of the linear and cubic terms in the above equation is of no importance; they will vanish when we take their expectation because  $\mathbf{y} - \mathbf{Ax}$  is Gaussian-distributed with zero mean and diagonal covariance. The expectation value of  $\|\mathbf{y} - \mathbf{Ax}\|_{\ell_2}^2$  is  $m(\sigma_e^2 \mathbf{x}^T \mathbf{x} + \sigma_n^2)$ , while for  $\|\mathbf{y} - \mathbf{Ax}\|_{\ell_2}^4$  the expectation will be  $(m^2 + 2m)(\sigma_e^2 \mathbf{x}^T \mathbf{x} + \sigma_n^2)^2$ , which can be seen from the fact that for a series of i.i.d. zero-mean Gaussian random variables  $w_1, \dots, w_k$  with the same variance  $q^2$ , one has

$$\begin{aligned} E[(w_1^2 + \dots + w_k^2)^2] &= E \left[ \sum_{i=1}^k w_i^4 + 2 \sum_{i=1}^k \sum_{j=i+1}^k w_i^2 w_j^2 \right] \\ &= \sum_{i=1}^k E[w_i^4] + 2 \sum_{i=1}^k \sum_{j=i+1}^k E[w_i^2 w_j^2] \\ &= k \cdot 3q^4 + 2 \cdot \frac{k(k-1)}{2} (q^2)^2 = (k^2 + 2k)q^4, \end{aligned} \quad (57)$$

where the fact from elementary probability theory that  $E[w_i^4] = 3q^4$  is used. By taking the expectation of (56), and

recalling the covariance matrix of  $\mathbf{y} - \mathbf{Ax} = \mathbf{Ex} + \mathbf{n}$ , it can be shown that

$$\begin{aligned} \mathbf{J}(\mathbf{x}) &= \frac{m^2 \sigma_e^4}{(\sigma_e^2 \mathbf{x}^T \mathbf{x} + \sigma_n^2)^2} \mathbf{xx}^T - \frac{2m^2 \sigma_e^4}{(\sigma_e^2 \mathbf{x}^T \mathbf{x} + \sigma_n^2)^2} \mathbf{xx}^T \\ &\quad + \frac{1}{\sigma_e^2 \mathbf{x}^T \mathbf{x} + \sigma_n^2} \mathbf{A}^T \mathbf{A} + \frac{(m^2 + 2m) \sigma_e^4}{(\sigma_e^2 \mathbf{x}^T \mathbf{x} + \sigma_n^2)^2} \mathbf{xx}^T \\ &= \frac{1}{\sigma_e^2 \mathbf{x}^T \mathbf{x} + \sigma_n^2} \mathbf{A}^T \mathbf{A} + \frac{2m \sigma_e^4}{(\sigma_e^2 \mathbf{x}^T \mathbf{x} + \sigma_n^2)^2} \mathbf{xx}^T, \end{aligned}$$

which is exactly (14).

## APPENDIX B PROOF OF PROPOSITION 2

Given the support  $S$ , the subspace  $\mathcal{F}$  is given by

$$\mathcal{F} = \text{span}(\{\mathbf{e}_{S_1}, \dots, \mathbf{e}_{S_s}\}),$$

therefore the unbiasedness in the neighborhood of  $\mathbf{x} \in \{\mathbf{u} : \text{supp}(\mathbf{u}) = S\}$  only requires that the bias function  $b(\mathbf{x}) = E[\hat{\mathbf{x}}_{\text{pinv}} - \mathbf{x}]$  is zero on  $\{\mathbf{u} : \text{supp}(\mathbf{u}) = S\}$ . It can be seen that for any  $\mathbf{x}$  whose support is  $S$ , one has

$$\begin{aligned} (E[\hat{\mathbf{x}}_{\text{pinv}}(\mathbf{y})])_S &= E[\mathbf{A}_S^\dagger \mathbf{y}] = E[\mathbf{A}_S^\dagger (\mathbf{A}_S \mathbf{x}_S + \mathbf{Ex} + \mathbf{n})] \\ &= \mathbf{A}_S^\dagger \mathbf{A}_S \mathbf{x}_S + \mathbf{A}_S^\dagger E[\mathbf{E}] \mathbf{x} + \mathbf{A}_S^\dagger E[\mathbf{n}] \\ &= \mathbf{x}_S, \end{aligned} \quad (58)$$

and

$$(E[\hat{\mathbf{x}}_{\text{pinv}}(\mathbf{y})])_{S^c} = E[(\hat{\mathbf{x}}_{\text{pinv}}(\mathbf{y}))_{S^c}] = 0. \quad (59)$$

Thus one has

$$E[\hat{\mathbf{x}}_{\text{pinv}}(\mathbf{y})] = \mathbf{x}, \quad \forall \mathbf{x} \in \{\mathbf{u} : \text{supp}(\mathbf{u}) = S\}. \quad (60)$$

The MSE of the oracle pseudoinverse estimator  $\hat{\mathbf{x}}_{\text{pinv}}$  for  $\mathbf{x} \in \{\mathbf{u} : \text{supp}(\mathbf{u}) = S\}$  equals that of the oracle estimator, which could be found, for instance, in [3], [20].

## APPENDIX C PROOF OF THEOREM 3

Assumption 1 implies that the eigenvalues of  $\mathbf{A}_S^T \mathbf{A}_S$ , denoted by  $\lambda_i$ , are bounded as follows

$$1 - \vartheta_{1,s} \leq \lambda_i \leq 1 + \vartheta_{u,s}, \quad i = 1, \dots, s. \quad (61)$$

Therefore the eigenvalues of  $(\mathbf{A}_S^T \mathbf{A}_S)^{-1}$ , denoted by  $\tilde{\lambda}_i$ , are bounded as follows

$$\frac{1}{1 + \vartheta_{u,s}} \leq \tilde{\lambda}_i \leq \frac{1}{1 - \vartheta_{1,s}}. \quad (62)$$

One can further derive from the above inequalities that

$$\begin{aligned} \frac{\|\mathbf{x}\|_{\ell_2}^2}{(1 + \vartheta_{u,s})^2} &\leq \|(\mathbf{A}_S^T \mathbf{A}_S)^{-1} \mathbf{x}_S\|_{\ell_2}^2 \leq \frac{\|\mathbf{x}\|_{\ell_2}^2}{(1 - \vartheta_{1,s})^2} \\ \frac{\|\mathbf{x}\|_{\ell_2}^2}{1 + \vartheta_{u,s}} &\leq \mathbf{x}_S^T (\mathbf{A}_S^T \mathbf{A}_S)^{-1} \mathbf{x}_S \leq \frac{\|\mathbf{x}\|_{\ell_2}^2}{1 - \vartheta_{1,s}} \end{aligned}$$



Substituting these inequalities into (27), one will obtain

$$\begin{aligned} d_{\text{CCRB}} &\leq \sigma_{\mathbf{x}}^2 \cdot \frac{1 + \vartheta_{u,s}}{(1 - \vartheta_{l,s})^2} \\ &\quad \times \frac{2m\sigma_e^2}{1 + 2m\sigma_e^2 + \vartheta_{u,s} + \frac{c_n(1+\vartheta_{u,s})}{m\sigma_e^2}}, \\ d_{\text{CCRB}} &\geq \sigma_{\mathbf{x}}^2 \cdot \frac{1 - \vartheta_{l,s}}{(1 + \vartheta_{u,s})^2} \\ &\quad \times \frac{2m\sigma_e^2}{1 + 2m\sigma_e^2 - \vartheta_{l,s} + \frac{c_n(1-\vartheta_{l,s})}{m\sigma_e^2}}. \end{aligned} \quad (63)$$

Next we wish to bound the term  $m\sigma_e^2$ . It can be seen from the definition of the perturbation level  $c_e$  that

$$m\sigma_e^2 = c_e \frac{\text{tr}(\mathbf{A}_S^T \mathbf{A}_S)}{s}. \quad (64)$$

With the help of (61), the bounds of  $m\sigma_e^2$  can be readily given by

$$c_e(1 - \vartheta_{l,s}) \leq m\sigma_e^2 \leq c_e(1 + \vartheta_{u,s}). \quad (65)$$

Substituting this into (63), one will obtain the bounds given by (28) and (29).

The bounds of  $\gamma_{\text{CCRB}}$  can also be derived by similar techniques. One will get the bounds of (30) and (31) by only substituting the following inequalities into (28) and (29):

$$\frac{s}{1 + \vartheta_{u,s}} \leq \text{tr}((\mathbf{A}_S^T \mathbf{A}_S)^{-1}) \leq \frac{s}{1 - \vartheta_{l,s}}. \quad (66)$$

#### APPENDIX D PROOF OF LEMMA 2

We first refer to [23] for the definition of the multivariate HCRB.

*Proposition 3:* [23] Suppose  $p(\mathbf{y}; \mathbf{x})$  are a class of pdf's parameterized by  $\mathbf{x} \in \mathcal{X}$ , and let  $\mathbf{x}, \mathbf{x} + \mathbf{v}_1, \dots, \mathbf{x} + \mathbf{v}_k$  be test points contained in the constrained parameter set  $\mathcal{X}$ . Define

$$\delta_i \mathbf{m}_{\mathbf{x}} = \mathbf{m}_{\mathbf{x} + \mathbf{v}_i} - \mathbf{m}_{\mathbf{x}}, \quad i = 1, \dots, k \quad (67)$$

$$\delta \mathbf{m}_{\mathbf{x}} = [\delta_1 \mathbf{m}_{\mathbf{x}}, \dots, \delta_k \mathbf{m}_{\mathbf{x}}] \quad (68)$$

$$\delta_i p = p(\mathbf{y}; \mathbf{x} + \mathbf{v}_i) - p(\mathbf{y}; \mathbf{x}), \quad (69)$$

$$\delta p = [\delta_1 p, \dots, \delta_k p]^T. \quad (70)$$

where  $\mathbf{m}_{\mathbf{x}} \in \mathbb{R}^n$  is a vector-valued function of  $\mathbf{x}$ . Then for any estimator  $\hat{\mathbf{x}}$  with mean  $\mathbf{m}_{\mathbf{x}}$ , i.e.  $E_{\mathbf{y}; \mathbf{x}}[\hat{\mathbf{x}}] = \mathbf{m}_{\mathbf{x}}$ , the estimator covariance matrix  $\text{Cov}(\hat{\mathbf{x}})$  satisfies the matrix inequality

$$\text{Cov}(\hat{\mathbf{x}}) \succeq \delta \mathbf{m}_{\mathbf{x}} \left\{ E_{\mathbf{y}; \mathbf{x}} \left[ \frac{\delta p \delta p^T}{p} \right] \right\}^\dagger \delta \mathbf{m}_{\mathbf{x}}^T, \quad (71)$$

where  $p$  denotes  $p(\mathbf{y}; \mathbf{x})$  for short.

Next Proposition 3 will be applied to the sparse estimation problem with general perturbation. For unbiased estimators, it is easily seen that  $\mathbf{m}_{\mathbf{x}} = \mathbf{x}$ , and thus the matrix  $\delta \mathbf{m}_{\mathbf{x}}$  equals  $\mathbf{V} = [\mathbf{v}_1, \dots, \mathbf{v}_k]$ . For the matrix

$$\mathbf{H} = E_{\mathbf{y}; \mathbf{x}} \left[ \frac{\delta p \delta p^T}{p} \right], \quad (72)$$

its  $(i, j)$ th element is given by

$$\begin{aligned} H_{ij} &= E_{\mathbf{y}; \mathbf{x}} \left[ \frac{\delta_i p}{p} \frac{\delta_j p}{p} \right] \\ &= E_{\mathbf{y}; \mathbf{x}} \left[ \left( \frac{p(\mathbf{y}; \mathbf{x} + \mathbf{v}_i)}{p(\mathbf{y}; \mathbf{x})} - 1 \right) \left( \frac{p(\mathbf{y}; \mathbf{x} + \mathbf{v}_j)}{p(\mathbf{y}; \mathbf{x})} - 1 \right) \right] \\ &= E_{\mathbf{y}; \mathbf{x}} \left[ \frac{p(\mathbf{y}; \mathbf{x} + \mathbf{v}_i) p(\mathbf{y}; \mathbf{x} + \mathbf{v}_j)}{p^2(\mathbf{y}; \mathbf{x})} \right] \\ &\quad - E_{\mathbf{y}; \mathbf{x}} \left[ \frac{p(\mathbf{y}; \mathbf{x} + \mathbf{v}_i)}{p(\mathbf{y}; \mathbf{x})} \right] - E_{\mathbf{y}; \mathbf{x}} \left[ \frac{p(\mathbf{y}; \mathbf{x} + \mathbf{v}_j)}{p(\mathbf{y}; \mathbf{x})} \right] + 1. \end{aligned} \quad (73)$$

The second term of the above equation is

$$-E_{\mathbf{y}; \mathbf{x}} \left[ \frac{p(\mathbf{y}; \mathbf{x} + \mathbf{v}_i)}{p(\mathbf{y}; \mathbf{x})} \right] = -\int_{\mathbb{R}^m} p(\mathbf{y}; \mathbf{x} + \mathbf{v}_i) d\mathbf{y} = -1, \quad (74)$$

and similarly the third term also equals  $-1$ . The first term is

$$\begin{aligned} &E_{\mathbf{y}; \mathbf{x}} \left[ \frac{p(\mathbf{y}; \mathbf{x} + \mathbf{v}_i) p(\mathbf{y}; \mathbf{x} + \mathbf{v}_j)}{p^2(\mathbf{y}; \mathbf{x})} \right] \\ &= \int_{\mathbb{R}^m} \frac{p(\mathbf{y}; \mathbf{x} + \mathbf{v}_i) p(\mathbf{y}; \mathbf{x} + \mathbf{v}_j)}{p(\mathbf{y}; \mathbf{x})} d\mathbf{y} \\ &= \left( \frac{\sigma_{\mathbf{x}}^2}{2\pi\sigma_{\mathbf{x}+\mathbf{v}_i}^2\sigma_{\mathbf{x}+\mathbf{v}_j}^2} \right)^{\frac{m}{2}} \exp \left( -\frac{\|\mathbf{A}\mathbf{v}_i\|_{\ell_2}^2}{2\sigma_{\mathbf{x}+\mathbf{v}_i}^2} - \frac{\|\mathbf{A}\mathbf{v}_j\|_{\ell_2}^2}{2\sigma_{\mathbf{x}+\mathbf{v}_j}^2} \right) \\ &\quad \times \int_{\mathbb{R}^m} \exp \left[ \left( \frac{\mathbf{v}_i^T \mathbf{A}^T}{\sigma_{\mathbf{x}+\mathbf{v}_i}^2} + \frac{\mathbf{v}_j^T \mathbf{A}^T}{\sigma_{\mathbf{x}+\mathbf{v}_j}^2} \right) (\mathbf{y} - \mathbf{A}\mathbf{x}) \right. \\ &\quad \left. - \frac{\|\mathbf{y} - \mathbf{A}\mathbf{x}\|_{\ell_2}^2}{2\zeta_{\mathbf{x}, \mathbf{v}_i, \mathbf{v}_j}^2} \right] d\mathbf{y} \\ &= \left( \frac{\sigma_{\mathbf{x}}^2 \zeta_{\mathbf{x}, \mathbf{v}_i, \mathbf{v}_j}^2}{\sigma_{\mathbf{x}+\mathbf{v}_i}^2 \sigma_{\mathbf{x}+\mathbf{v}_j}^2} \right)^{\frac{m}{2}} \exp \left[ -\frac{\|\mathbf{A}\mathbf{v}_i\|_{\ell_2}^2}{2\sigma_{\mathbf{x}+\mathbf{v}_i}^2} - \frac{\|\mathbf{A}\mathbf{v}_j\|_{\ell_2}^2}{2\sigma_{\mathbf{x}+\mathbf{v}_j}^2} \right. \\ &\quad \left. + \frac{\zeta_{\mathbf{x}, \mathbf{v}_i, \mathbf{v}_j}^2}{2} \left\| \frac{\mathbf{A}\mathbf{v}_i}{\sigma_{\mathbf{x}+\mathbf{v}_i}^2} + \frac{\mathbf{A}\mathbf{v}_j}{\sigma_{\mathbf{x}+\mathbf{v}_j}^2} \right\|_{\ell_2}^2 \right], \end{aligned} \quad (75)$$

where

$$\frac{1}{\zeta_{\mathbf{x}, \mathbf{v}_i, \mathbf{v}_j}^2} = \frac{1}{\sigma_{\mathbf{x}+\mathbf{v}_i}^2} + \frac{1}{\sigma_{\mathbf{x}+\mathbf{v}_j}^2} - \frac{1}{\sigma_{\mathbf{x}}^2}. \quad (76)$$

Substituting these results into (73), one will readily obtain (37), and Lemma 2 is proved.

#### APPENDIX E PROOF OF THEOREM 4

For simplicity, it is assumed without loss of generality that the support of  $\mathbf{x}$  is  $S = \{1, 2, \dots, s\}$ . We split the MSE of an estimator  $\hat{\mathbf{x}}$  into two parts as follows:

$$\text{mse}(\hat{\mathbf{x}}) = \sum_{i \in S} E[(\hat{x}_i - x_i)^2] + \sum_{i \notin S} E[(\hat{x}_i - x_i)^2], \quad (77)$$

i.e. the support part and the non-support part. We choose different sets of  $\mathbf{v}_i$  for the two parts respectively, and in the end combine these two parts to get a lower bound. This approach results from the fact that the MSE of a vector-valued estimator is the sum of the MSE of its components.

For the lower bound of the support part, the following  $\{\mathbf{v}_i\}_{i=1}^s$  is employed:

$$\mathbf{v}_i = t\mathbf{e}_i, \quad i = 1, \dots, s, \quad (78)$$

where  $t$  is an arbitrary real number. After the corresponding covariance matrix is obtained, we take the limit  $t \rightarrow 0$  and afterwards take the sum of only the first  $s$  diagonal elements to obtain the lower bound of the support part. It can be proved (see Appendix F) that this lower bound is identical to the CCRB.

For the non-support part, a different set of testing points are used. As mentioned before, when one of the nonzero elements is small, the HCRB should be larger than the CCRB, and thus the nonzero components of small magnitude should be taken into consideration when constructing the set of  $\mathbf{v}_i$ . The following  $\{\mathbf{v}_i\}_{i=1}^{n-s+1}$  is used:

$$\mathbf{v}_i = \begin{cases} x_q \mathbf{e}_{i+s} - x_q \mathbf{e}_q, & i = 1, \dots, n-s, \\ t \mathbf{e}_q, & i = n-s+1. \end{cases} \quad (79)$$

Here  $t$  is also an arbitrary real number which will tend to zero after the covariance matrix is obtained. It is obvious that such  $\{\mathbf{v}_i\}$  will not violate the sparsity of the testing points  $\{\mathbf{x} + \mathbf{v}_i\}$ . After the limit  $t \rightarrow 0$  is taken, the last  $n-s$  diagonal elements of the covariance matrix will be summed to represent the lower bound of the non-support part.

The matrix  $\mathbf{V}$  in (35) could be expressed as

$$\mathbf{V} = \begin{bmatrix} t & -x_q & -x_q & -x_q \\ 0 & x_q & & 0 \\ \vdots & & \ddots & \\ 0 & 0 & & x_q \end{bmatrix} = \begin{bmatrix} t & -x_q \mathbf{1}^T \\ \mathbf{0} & x_q \mathbf{U}_{n-s} \end{bmatrix}, \quad (80)$$

(we have slightly changed the order of  $\mathbf{v}_i$ 's which has no effect on the final result), where the bold face  $\mathbf{1}$  denotes the column vector  $[1, 1, \dots, 1]^T$ . Next we have to compute the elements of the matrix  $\mathbf{H}$ , which are given as follows:

$$H_{11} = \left( \frac{\sigma_{\mathbf{x}}^2 \zeta_{\mathbf{x},q}^2}{\sigma_q^4} \right)^{\frac{n}{2}} \exp \left( \frac{t^2}{\sigma_q^2} \left( 2 \frac{\zeta_{\mathbf{x},q}^2}{\sigma_q^2} - 1 \right) \right) - 1, \quad (81)$$

where it has been defined that

$$\begin{aligned} \sigma_q^2 &= \sigma_n^2 + \sigma_e^2 (\|\mathbf{x} + t \mathbf{e}_q\|_{\ell_2}^2), \\ \zeta_{\mathbf{x},q}^2 &= \left( \frac{2}{\sigma_q^2} - \frac{1}{\sigma_{\mathbf{x}}^2} \right)^{-1}, \end{aligned} \quad (82)$$

and

$$H_{1i} = H_{i1} = \exp \left( -\frac{tx_q}{\sigma_{\mathbf{x}}^2} + \frac{x_q^2}{\sigma_{\mathbf{x}}^2} \left( \frac{\sigma_q^2}{\sigma_{\mathbf{x}}^2} - 1 \right) \right) - 1, \quad (83)$$

$$i = 2, \dots, n-s+1,$$

$$H_{ij} = \exp \left( \frac{(1 + \delta_{ij})x_q^2}{\sigma_{\mathbf{x}}^2} \right) - 1, \quad (84)$$

$$i, j = 2, \dots, n-s+1.$$

The matrix  $\mathbf{H}$  could be represented as

$$\mathbf{H} = \begin{bmatrix} a(t) & b(t) \mathbf{1}^T \\ b(t) \mathbf{1} & \mathbf{D} \end{bmatrix}, \quad (85)$$

where  $a(t) = H_{11}$ ,  $b(t) = H_{12}$  and  $\mathbf{D} = (H_{22} - H_{23})\mathbf{U}_{n-s} + H_{23}\mathbf{1}\mathbf{1}^T$ . In order to check the existence and the expression

of  $\mathbf{H}^{-1}$ , we first calculate the inverse of  $\mathbf{D}$  by the Sherman-Morrison formula [33]:

$$\mathbf{D}^{-1} = \frac{1}{H_{22} - H_{23}} \left( \mathbf{U}_{n-s} - \frac{H_{23}}{H_{22} + H_{23}(n-s-1)} \mathbf{1}\mathbf{1}^T \right). \quad (86)$$

Then the blockwise inversion formula is used for the calculation of  $\mathbf{H}^{-1}$  (if it exists):

$$\mathbf{H}^{-1} = \begin{bmatrix} f_{11}(t) & f_{12}(t) \mathbf{1}^T \\ f_{12}(t) \mathbf{1} & \mathbf{D}^{-1} + \frac{b^2(t) \mathbf{D}^{-1} \mathbf{1}\mathbf{1}^T \mathbf{D}^{-1}}{a(t) - b^2(t) \mathbf{1}^T \mathbf{D}^{-1} \mathbf{1}} \end{bmatrix}, \quad (87)$$

where  $f_{11}(t)$  and  $f_{12}(t)$  are some functions of  $t$ . Because at last only the last  $n-s$  diagonal elements will be summed up, the specific form of the two functions are of no importance. The existence of  $\mathbf{H}^{-1}$  relies on whether the submatrices are valid. By employing (86), one has

$$\begin{aligned} \mathbf{D}^{-1} \mathbf{1} &= \frac{1}{H_{22} + H_{23}(n-s-1)} \mathbf{1} \\ \mathbf{1}^T \mathbf{D}^{-1} \mathbf{1} &= \frac{n-s}{H_{22} + H_{23}(n-s-1)}. \end{aligned} \quad (88)$$

With these equations, it can be shown by tedious calculation that

$$\begin{aligned} & \lim_{t \rightarrow 0} \frac{b^2(t) \mathbf{D}^{-1} \mathbf{1}\mathbf{1}^T \mathbf{D}^{-1}}{a(t) - b^2(t) \mathbf{1}^T \mathbf{D}^{-1} \mathbf{1}} \\ &= \frac{\beta(1 - 2\sigma_e^2 \beta)^2}{H_{22} + H_{23}(n-s-1)} \\ & \quad \times ([H_{22} + H_{23}(n-s-1)](1 + 2n\sigma_e^4 \beta) \\ & \quad - (n-s)\beta(1 - 2\sigma_e^2 \beta)^2)^{-1}, \end{aligned} \quad (89)$$

and that

$$\begin{aligned} \mathbf{H}_{22} &\equiv \lim_{t \rightarrow 0} \left( \mathbf{D}^{-1} + \frac{b^2(t) \mathbf{D}^{-1} \mathbf{1}\mathbf{1}^T \mathbf{D}^{-1}}{a(t) - b^2(t) \mathbf{1}^T \mathbf{D}^{-1} \mathbf{1}} \right) \\ &= \frac{(n-s) \exp(-\beta)}{\exp \beta - 1} \times \left( 1 - \frac{1}{n-s + \exp \beta (1 - g(\beta))^{-1}} \right), \end{aligned} \quad (90)$$

where we have defined  $\mathbf{H}_{22}$  as the limit of the  $(2, 2)$ th submatrix of  $\mathbf{H}$ , and the function  $g(\beta)$  is defined as (40). As will be shown later, under the modest requirement that  $n \geq 2$ , for any  $\beta > 0$  one has  $0 < g(\beta) < 1$ , and thus the expressions presented above are all valid. In this way we have not only checked the invertibility of  $\mathbf{H}$ , but also find out the expression of the inversion's limit.

To get the final form of the HCRB, we calculate  $\mathbf{V}\mathbf{H}^{-1}\mathbf{V}^T$  and sum up its last  $n-s$  diagonal elements. By straightforward calculation it can be verified that this is just equal to  $x_q^2 \text{tr}(\mathbf{H}_{22})$ . Adding this to the lower bound of the support part, given by

$$\begin{aligned} \sum_{i \in S} E[(\hat{x}_i - x_i)^2] &\geq \text{CCRB}_{\max} \sup \\ &= \sigma_{\mathbf{x}}^2 \left( s - \frac{2m\sigma_e^4 \|\mathbf{x}\|_{\ell_2}^2}{\sigma_{\mathbf{x}}^2 + 2m\sigma_e^4 \|\mathbf{x}\|_{\ell_2}^2} \right), \end{aligned} \quad (91)$$

one will finally get the expression (39).

The last part of this section deals with the properties of  $g(\beta)$ . The proof of the two limits given by (42) is straightforward. In order to prove (41), we consider separately the situations

$0 < \beta \leq 1/2\sigma_e^2$  and  $\beta > 1/2\sigma_e^2$ . When  $0 < \beta \leq 1/2\sigma_e^2$ , one has

$$(1 - 2\sigma_e^2\beta)^2 < 1 < 1 + 2n\sigma_e^4\beta,$$

and together with  $\beta < \exp \beta - 1$ , it leads to the inequality that  $g(\beta) < 1$ . When  $\beta > 1/2\sigma_e^2$ , it follows that

$$\begin{aligned} \frac{\beta}{\exp \beta - 1} \frac{(1 - 2\sigma_e^2\beta)^2}{1 + 2n\sigma_e^4\beta} &< \frac{\beta}{\exp \beta - 1} \frac{4\sigma_e^4\beta^2}{2n\sigma_e^4\beta} \\ &= \frac{2}{n} \frac{\beta^2}{\exp \gamma - 1}. \end{aligned}$$

Because  $\beta^2/(\exp \gamma - 1) < 1$  for all  $\beta > 0$ , it can be seen that  $g(\beta) < 1$  when  $n \geq 2$ . Combining the discussions of the two situations, we have proved that  $g(\beta) < 1$  for all  $\beta > 0$ . The inequality that  $g(\beta) \geq 0$  for all  $\beta > 0$  is trivial.

## APPENDIX F

### LOWER BOUND OF THE SUPPORT PART

In this section, we prove that the lower bound of the support part obtained by using  $\mathbf{v}_i = t\mathbf{e}_i, i = 1, \dots, s$  and taking  $t \rightarrow 0$  is just the CCRB of maximal support. It can be easily seen that the matrix  $\delta\mathbf{m}_\mathbf{x}$  in (68) is

$$\delta\mathbf{m}_\mathbf{x} = t \begin{bmatrix} \mathbf{U}_s \\ \mathbf{0} \end{bmatrix}, \quad (92)$$

therefore the right side of (71) is

$$\delta\mathbf{m}_\mathbf{x} \mathbf{H} \delta\mathbf{m}_\mathbf{x}^\mathbf{T} = \begin{bmatrix} t^2 \mathbf{H}^\dagger & \mathbf{0} \\ \mathbf{0} & \mathbf{0} \end{bmatrix}, \quad (93)$$

where the matrix  $\mathbf{H}$  is given by (72). Next we calculate the limit of  $\mathbf{H}/t^2$ . It can be seen that

$$\frac{1}{t^2} \mathbf{H} = E \left[ \frac{\delta p}{pt} \frac{\delta p^\mathbf{T}}{pt} \right], \quad (94)$$

and for  $\delta p/pt$ , one has

$$\left( \frac{\delta p}{pt} \right)_i = \frac{1}{p(\mathbf{y}; \mathbf{x})} \frac{p(\mathbf{y}; \mathbf{x} + t\mathbf{e}_i) - p(\mathbf{y}; \mathbf{x})}{t}. \quad (95)$$

Taking the limit  $t \rightarrow 0$ , one has

$$\begin{aligned} \lim_{t \rightarrow 0} \left( \frac{\delta p}{pt} \right)_i &= \frac{1}{p(\mathbf{y}; \mathbf{x})} \lim_{t \rightarrow 0} \frac{p(\mathbf{y}; \mathbf{x} + t\mathbf{e}_i) - p(\mathbf{y}; \mathbf{x})}{t} \\ &= \frac{1}{p(\mathbf{y}; \mathbf{x})} \frac{\partial p(\mathbf{y}; \mathbf{x})}{\partial \mathbf{e}_i} = \frac{\partial \ln p(\mathbf{y}; \mathbf{x})}{\partial \mathbf{e}_i}, \end{aligned} \quad (96)$$

where  $\partial/\partial \mathbf{e}_i$  denotes the directional derivative along  $\mathbf{e}_i$  with respect to  $\mathbf{x}$ . Thus the limit of  $\delta p/pt$  is

$$\lim_{t \rightarrow 0} \frac{\delta p}{pt} = [\mathbf{U}_s \quad \mathbf{0}] \nabla_\mathbf{x} \ln p(\mathbf{y}; \mathbf{x}), \quad (97)$$

and the limit of  $\mathbf{H}/t^2$  is

$$\begin{aligned} \lim_{t \rightarrow 0} \frac{1}{t^2} \mathbf{H} &= E \left[ \lim_{t \rightarrow 0} \frac{\delta p}{pt} \frac{\delta p^\mathbf{T}}{pt} \right] \\ &= [\mathbf{U}_s \quad \mathbf{0}] E \left[ (\nabla_\mathbf{x} \ln p(\mathbf{y}; \mathbf{x})) (\nabla_\mathbf{x}^\mathbf{T} \ln p(\mathbf{y}; \mathbf{x})) \right] \begin{bmatrix} \mathbf{U}_s \\ \mathbf{0} \end{bmatrix} \\ &= [\mathbf{U}_s \quad \mathbf{0}] \mathbf{J} \begin{bmatrix} \mathbf{U}_s \\ \mathbf{0} \end{bmatrix}. \end{aligned} \quad (98)$$

Here the matrix  $\mathbf{J}$  is just the Fisher information matrix, and thus it can be verified that the above matrix is invertible in the setting given by Section II. Substituting it into (93), and take the sum of the first  $s$  diagonal elements, one will get

$$\lim_{t \rightarrow 0} \text{tr}(t^2 \mathbf{H}^{-1}) = \text{tr} \left( \left( \begin{bmatrix} \mathbf{U}_s & \mathbf{0} \end{bmatrix} \mathbf{J} \begin{bmatrix} \mathbf{U}_s \\ \mathbf{0} \end{bmatrix} \right)^{-1} \right). \quad (99)$$

Comparing this with the proof of Theorem 1, one will readily accept that the bound obtained is just the CCRB for maximal support case.

## REFERENCES

- [1] D. L. Donoho, M. Elad, and V. N. Temlyakov, "Stable recovery of sparse overcomplete representations in the presence of noise," *IEEE Trans. Inf. Theory*, vol. 52, no. 1, pp. 6-18, Jan. 2006.
- [2] J. A. Tropp, "Just relax: convex programming methods for identifying sparse signals in noise," *IEEE Trans. Inf. Theory*, vol. 52, no. 3, pp. 1030-1051, Mar. 2006.
- [3] E. Candès and T. Tao, "The Dantzig selector: Statistical estimation when  $p$  is much larger than  $n$ ," *Ann. Statist.*, vol. 35, no. 6, pp. 2313-2351, Dec. 2007.
- [4] J. Tropp and A. Gilbert, "Signal recovery from partial information via orthogonal matching pursuit," *IEEE Trans. Inf. Theory*, vol. 53, no. 12, pp. 4655-4666, Dec. 2007.
- [5] D. Needell and R. Vershynin, "Uniform uncertainty principle and signal recovery via regularized orthogonal matching pursuit," *Found. Comput. Math.*, vol. 9, no. 3, pp. 317-334, June 2009.
- [6] D. Needell and J. A. Tropp, "CoSaMP: Iterative signal recovery from noisy samples," *Appl. Comput. Harmon. Anal.*, vol. 26, no. 3, pp. 301-321, 2009.
- [7] W. Dai and O. Milenkovic, "Subspace pursuit for compressive sensing signal reconstruction," *IEEE Trans. Inf. Theory*, vol. 55, no. 5, pp. 2230-2249, May 2009.
- [8] T. Blumensath and M. Davies, "Iterative hard thresholding for compressed sensing," *Appl. Comput. Harmon. Anal.*, vol. 27, no. 3, pp. 265-274, Nov. 2009.
- [9] J. Jin, Y. Gu, and S. Mei, "A stochastic gradient approach on compressive sensing signal reconstruction based on adaptive filtering framework," *IEEE Journal of Selected Topics in Signal Process.*, vol. 4, no. 2, pp. 409-420, April 2010.
- [10] X. Wang, Y. Gu, and L. Chen, "Proof of convergence and performance analysis for sparse recovery via zero-Point attracting projection," *IEEE Trans. Signal Process.*, vol. 60, no. 8, pp. 4081-4093, Aug. 2012.
- [11] E. Candès, J. Romberg, and T. Tao, "Robust uncertainty principles: Exact signal reconstruction from highly incomplete frequency information," *IEEE Trans. Inf. Theory*, vol. 52, no. 2, pp. 489-509, Feb. 2006.
- [12] D. L. Donoho, "Compressed sensing," *IEEE Trans. Inf. Theory*, vol. 52, no. 4, pp. 1289-1306, Apr. 2006.
- [13] E. Candès and M. B. Wakin, "An introduction to compressive sampling," *IEEE Signal Process. Mag.*, vol. 25, pp. 21-30, 2008.
- [14] E. Candès, J. Romberg, and T. Tao, "Stable signal recovery from incomplete and inaccurate measurements," *Comm. Pure Appl. Math.*, vol. 59, no. 8, pp. 1207-1223, 2006.
- [15] R. Saab, R. Chartrand, and O. Yilmaz, "Stable sparse approximations via nonconvex optimization," *ICASSP 2008*, pp. 3885-3888, Mar. 2008.
- [16] T. T. Cai, L. Wang, and G. Xu, "Stable recovery of sparse signals and an oracle inequality," *IEEE Trans. Inf. Theory*, vol. 56, no. 7, pp. 3516-3522, July 2010.
- [17] T. T. Cai and L. Wang, "Orthogonal matching pursuit for sparse signal recovery with noise," *IEEE Trans. Inf. Theory*, vol. 57, no. 7, pp. 4680-4688, July 2011.
- [18] D. Needell and R. Vershynin, "Signal recovery from incomplete and inaccurate measurements via regularized orthogonal matching pursuit," *IEEE Journal of Selected Topics in Signal Process.*, vol. 4, no. 2, pp. 310-316, Apr. 2010.
- [19] E. Candès and M. A. Davenport, "How well can we estimate a sparse vector?" *Appl. Comput. Harmon. Anal.*, available online Aug. 2012.
- [20] Z. Ben-Haim and Y. C. Eldar, "The Cramér-Rao bound for estimating a sparse parameter vector," *IEEE Trans. Signal Process.*, vol. 58, no. 6, pp. 3384-3389, Jun. 2010.
- [21] E. L. Lehmann and G. Casella, *Theory of Point Estimation*, 2nd ed. New York: Springer-Verlag, 1998.

- [22] S. M. Kay, *Fundamentals of Statistical Signal Processing: Estimation Theory*. Englewood Cliffs, NJ: Prentice-Hall, 1993.
- [23] J. D. Gorman and A. O. Hero, "Lower bounds for parametric estimation with constraints," *IEEE Trans. Inf. Theory*, vol. 36, no. 6, pp. 1285-1301, Nov. 1990.
- [24] D. G. Chapman and H. Robbins, "Minimum variance estimation without regularity assumptions," *The Annals of Mathematical Statistics*, vol. 22, no. 4, pp. 581-586, 1951.
- [25] E. W. Barankin, "Locally best unbiased estimates," *Ann. Math. Stat.*, vol. 20, no. 4, pp. 477-501, 1949.
- [26] Z. Ben-Haim and Y. C. Eldar, "On the constrained Cramér-Rao bound with a singular Fisher information matrix," *IEEE Signal Process. Lett.*, vol. 16, no. 6, pp. 453-456, Jun. 2009.
- [27] A. Jung, Z. Ben-Haim, F. Hlawatsch, and Y. C. Eldar, "Unbiased estimation of a sparse vector in white Gaussian noise," *IEEE Trans. Inf. Theory*, vol. 57, no. 12, pp. 7856-7876, Dec. 2011.
- [28] A. Hormati, A. Karbasi, S. Mohajer and M. Vetterli, "An estimation theoretic approach for sparsity pattern recovery in the noisy setting," arXiv preprint arXiv:0911.4880, 2009.
- [29] M. Herman and T. Strohmer, "General deviants: An analysis of perturbations in compressed sensing," *IEEE Journal of Selected Topics in Signal Process.*, vol. 4, no. 2, pp. 342-349, Apr. 2010.
- [30] H. Zhu, G. Leus, and G. Giannakis, "Sparsity-cognizant total least-squares for perturbed compressive sampling," *IEEE Trans. Signal Process.*, vol. 59, no. 5, pp. 2002-2016, May 2011.
- [31] J. Ding, L. Chen, and Y. Gu, "Perturbation analysis of orthogonal matching pursuit," accepted by *IEEE Trans. Signal Process.*, available online: <http://arxiv.org/abs/1106.3373>.
- [32] D. L. Donoho and M. Elad, "Optimally sparse representation in general (nonorthogonal) dictionaries via  $\ell_1$  minimization," *Proc. Nat. Acad. Sci.*, vol. 100, no. 5, pp. 2197-2202, Mar. 2003.
- [33] G. H. Golub and C. F. Van Loan, *Matrix Computations*, Johns Hopkins University Press, Baltimore, MD, 3rd edition, 1996.
- [34] E. Candès, "The restricted isometry property and its implications for compressed sensing," *Compte Rendus de l'Academie des Sciences*. Paris, France, 2008, vol. 346, pp. 589-592, ser. I.
- [35] E. Candès and T. Tao, "Decoding by linear programming," *IEEE Trans. Inf. Theory*, vol. 51, no. 12, pp. 4203-4215, Dec. 2005.
- [36] J. Blanchard, C. Cartis, and J. Tanner, "Compressed Sensing: How sharp is the Restricted Isometry Property," Apr. 2010, available online at <http://arxiv.org/abs/1004.5026>.
- [37] S. Schmutzhard, A. Jung, F. Hlawatsch, Z. Ben-Haim, and Y. C. Eldar, "A lower bound on the estimator variance for the sparse linear model," in *Proc. 44th Asilomar Conf. Signals, Systems, Computers*, Pacific Grove, CA, Nov. 2010.
- [38] Z. Ben-Haim, Y. Eldar, and M. Elad, "Coherence-based performance guarantees for estimating a sparse vector under random noise," *IEEE Trans. Signal Process.*, vol. 58, no. 10, pp. 5030-5043, Oct. 2010.